# PRATHAM
# IIT BOMBAY STUDENT SATELLITE

## Report
## Thermal Subsystem

By

**Pratham Team**



**Department of Aerospace Engineering,**

**Indian Institute of Technology, Bombay**
**February 2016**

# Contents

# List of Tables

# List of Figures

# Chapter 1

# Intoduction

The environment up to a height of around 500 km above the Earth is strongly affected by the presence of the denser layers of the atmosphere and by interaction with the hydrosphere, and thus experience relatively mild conditions of temperature. However, above 500 km, the atmosphere becomes too thin to moderate the ambient thermal conditions and consequently, the environment above such a height is prone to extremes of temperature, being directly exposed to solar radiation and deep space.

Spacecraft, which are primarily intended to perform scientific missions which require them to be positioned far away from the Earth's surface, spend their entire lifetime in the harsh environments of the upper atmosphere or interplanetary space. Being electromechanical systems, however, these spacecraft also have certain requirements of temperature ranges outside which their systems cannot function viably. Hence, every such spacecraft must incorporate a thermal subsystem to achieve an optimal thermal environment for its smooth functioning, through either active or passive means.

The requirements of thermal control and the challenges involved in realizing these in case of Nano satellites in Low Earth Orbit (LEO) are unique. The IIT Bombay Student Satellite, PRATHAM, belongs to this class of satellites, having a mass of less than 10 kg and orbiting in a LEO of approximate altitude of 500-600 km. The Thermals Subsystem of PRATHAM aims to maintain a cycle of temperature within the satellite which has a narrow range and lies around the normal terrestrial temperatures, minimize spatial gradients of temperature, dissipate excess heat generated by other subsystems and maintain sensitive components within their specified functional ranges of temperature

# Chapter 2

# Requirements Constraint Analysis

In this part we will discuss the requirements of other sub-systems which need to be addressed by the thermals subsystem. Allowed temperature range for different components on Pcbs

## 2.1 Requirements from Power Sub-System to Thermals Sub-System

- The optimal operating range of the battery is from $5^0$ C to $25^0$ C. The acceptable operating range is $0^0$ C to $35^0$ C. The thermals sub system shall try and maintain the battery within its optimal operating range. If that is not possible the battery must be maintained in the acceptable operating range.
- They shall remove the excessive heat from Power Circuits, since the temperature range of the components (industrial grade) is given in 2.1

## 2.2 Requirements from Communication and Ground Station Sub-System to Thermal subsystem

- Thermal sub-system will protect the monopoles from heating above $100^0$ C
- They shall remove the excessive heat from the 2 monopole circuits, since the temperature range of the components (industrial grade) is given in 2.1

## 2.3 Requirements from On Board Computer Sub-System to Thermals Sub-System

- They shall remove the excessive heat from the OBC circuits, so that its temperature is inside the temperature range of the components(industrial grade) is given in 2.1

The aim of the thermal subsystem is to satisfy all these requirements. The most stringent requirement is maintaining the temperature of the battery. In the next chapter we will look into the design procedure and performing the thermal analysis of the satellite

| | **Operating Range** | | **Storage Range** | |
|---|---|---|---|---|
| **Components/ Temperature ($^0$ C)** | **Min** | **Max** | **Min** | **Max** |
| Power Board | 0 | 70 | -40 | 125 |
| OBC Board | 0 | 70 | -65 | 150 |
| Sunsensor Board | -40 | 50 | -40 | 85 |
| RF Boards | 0 | 70 | -55 | 125 |
| Magnetometer | -40 | 70 | -55 | 125 |
| GPS Receiver | -25 | 65 | | |
| Battery | 0 | 35 | | |

Table 2.1: Operating Temperature

# Chapter 3

# Thermal Modeling

This chapter deals with the thermal modeling and simulation of the satellite, which would help us in determining the temperature of the various parts of the satellite. The thermal modeling and analysis has been done using the Siemens PLM Software NX Nastran 9.0. This software makes it easy to model nonlinear and transient heat transfer processes including conduction and radiation. Nastran uses finite element models (FEM) and highly accurate numerical methods for solving the element based thermal models. The thermals' scientist in ISAC associated with small satellites, Mr.Nagaraju helped us in the thermal modeling. The modeling involves specifying the geometric model of the various parts of the satellite, couplings and boundary conditions associated with it and the solution parameters required for solving the problem. The whole modeling process is explained in this chapter.

## 3.1 Modeling approach

### 3.1.1 Different Approach for Meshing Used

Thermal modeling of the satellite has been done in few steps.

1. **3-D meshing:**
   First of all complete SW model was imported in NASTRAN. All the internal components were removed. It contained satellite body made of six side panels connected through flanges and screws with each other. Four solar panels, four MLI between solar panels and satellite body. Screws and washers connecting solar panel and satellite body through MLI were present in the CAD model. Meshing was done using 3-D tetrahedral elements. Due to presence of screws, washers and holes, meshing was complex. For meshing, entire model was selected at a time so, element size was dependent on the dimension of the smallest object, in our case screws. Small element size further increased complexity of the mesh. It took two days to simulate for five orbits. Internal electrical components were still to be modeled. So, due to high computational time, other ways of modeling and meshing were tried in the next step.

2. **2-D meshing of polygon body:**
   In second step, a simplified CAD version of the satellite was made. In this model, satellite body was approximated as a hollow shell of thickness 3 mm. Four solar panels and four MLIs between solar panel and satellite body. Intricate feature like screws and washers were removed from this model so, there were no holes. Mesh collectors were defined for different components which contains material property and thickness of objects associated with it. Different components are then associated with corresponding mesh collector depending on their material and thickness.

All the components were meshed using "2-D meshing of polygon body". It converts a polygon body into shell of zero thickness. Such modeling can be used in case of slab like body or body of small thickness. In our case solar panel(3 mm), MLI(10 mm) and satellite body(2.5 mm) can be modeled like this because their thickness is very small as compared to other dimensions. It takes equivalent conduction into account between two parallel surfaces of slab. For this, heat transfer coefficient was defined in mesh collector which is given as K*A/L. Where 'K' is conductivity of material, 'A' is cross section area of slab and 'L' is thickness of the slab. In this case temperature gradient exists in two directions on all the surfaces. Temperature gradient in the direction of normal to surface is zero but temperature of two parallel surfaces perpendicular to direction of thickness will differ since, equivalent conduction has been taken into account. NASTRAN gave an error message of "improper geometry" and could not solve it. This method did not work but it was clear that absence of holes and other intricate features made meshing simpler.

3. **2-D mid surface meshing:**
   In the third step, same CAD model was used. Mid surface of all the components were created. Mesh collector was defined in similar way as previous. 2-D meshing with 'quad4' elements were done after associating components to corresponding mesh collector. In this case a single surface with zero thickness represents entire body. Temperature gradient exists only on the surface and temperature along direction of thickness is assumed to be constant. Meshing was much simpler in this case and computational time was reduced to great extent.

**Conclusion:** Meshing in 3-D is most complex while it is simplest in 2-D mid surface meshing. 2-D mid surface meshing has least number of nodes. But, 3-D meshing is closest to the actual scenario while 2-D mid surface is the least close. 2-D meshing of polygon body is little better approximation because it takes equivalent conduction between parallel surfaces into account. So, in the 2-D mid surface case results will deviate from that in 3-D case. This is due to the assumption that temperature is constant along the direction of thickness. Error in results will depend on the dimension of the object. If thickness of the body is small when compared to other dimensions, error will be less. Error will reduce as the thickness decreases.

### 3.1.2 Error Visualization:

To get an idea of how much error arises in case of 2-D meshing method, an analysis has been done for comparison between results of 3-D and 2-D meshing. Comparison has been done for a physical scenario: Three slabs of same size(100X100X10 $mm^3$) are parallel to each other at equal distance. Middle slab is connected to the right one by screws of cross section 10X10 $mm^2$. Right side of left slab and left side of middle slab as well as left side of right slab and right side of middle slab are involved in heat transaction. Left and right slabs are radiating to environment from its outermost surfaces. Middle slab is generating 10 W of heat. Ambient temperature is 20 $^0$C as well as initial temperature of body.

1. **CAD model:** For 2-D mid surface meshing, three slabs of cross section 100X100 $mm^2$ and thickness 10 mm is created. For 3-D meshing same arrangement of three slabs are used, in addition to that two of the slabs are connected by four stubs at four corners. Stubs cross section area is 10X10 $mm^2$ and lenght is also 10 mm.

2. **Meshing and modeling:** First model has been meshed using 2-D quad4 elements after creating mid surface of each slabs. Stubs are modeled using total conductance defined as K*A/L, Where 'K' is conductivity of stub, 'A' is cross section area of stub and 'L' is length of the stub, in this case 10 mm. Then radiation coupling is defined between both pairs of slabs using view factor. Radiation to environment is also defined from left and right slabs. Heat load of 10 W is applied on middle surface. Second model with stubs has been meshed using 3-D tetrahedral elements. Radiation coupling and radiation to environment is defined in similar way as previous. Internal heat generation of 1XE-4 $W/mm^3$ is applied on middle slab. Both the simulations have been done for 1000s using solver - 'NX THERMAL / FLOW' and solution type - 'Advanced Thermal'. Time step of 10s is used for each simulation.

3. **Result comparison:** Temperature of each slab is given after 1000s in each case:

| | Temperature ($^0$C) | |
|---|---|---|
| Slabs | 2-D | 3-D |
| Right | 32.74 | 32.32 |
| Middle | 34.18 | 34.1 |
| Left | 21.95 | 21.95 |

Table 3.1: Result Comparison

**Conclusion:** Difference in temperature of middle and left slab is negligible while that in right slab is relatively higher. That is due to heat capacity of stubs. From above simulation, it is clear that error in 2-D mid surface meshing is very low.

Considering accuracy of results and computational cost, 2-D mid surface meshing method is best suited for our purpose. Further simulations are done using 2-D mid surface meshing which is explained in detail below.

## 3.2 Final approach

For thermal modeling mid surface of all the components was created as most of the components - solar panel, satellite sides, pcbs, battery box have very small thickness which can be approximated as a surface. Then, thin shell property was defined for all the components for calculation of volume, mass and heat capacity. Few components like - magnetometer and GPS are of significant thickness, but these components are defined in similar way, because we need a rough idea of temperature of such components. So, for the sake of simplicity and reduce computational time these were modeled similar to other components.

## 3.3 Geometry

### 3.3.1 Satellite body

The Pratham satellite can be approximated as a cube of side length $\sim$ 260 mm. The satellite has six faces with the following terminology:
Side facing the Sun – Sunside
Side opposite to the sun facing side – ASS
Side facing the earth – Nadir
Side opposite to Nadir – Zenith
Side whose normal is aligned with the velocity vector – Leading
Side opposite leading – Lagging
Satellite body is assembly of six side panels connected through flanges. These sides are square of size 260 mm and thickness of is 2.5 mm. Satellite body is modeled as hollow cube of 2.5 mm thickness. After creating its mid surface, it is converted into hollow cube of zero thickness whose sides are not connected to their adjacent ones along edges. Then, Thin shell Property is defined for satellite body. Thin Shell Property implies that the face is modeled as a two dimensional plate with a very small thickness. In thermal point of view, the temperature gradient will be only along the plane of the face and there would not be any temperature gradient along the thickness of the face. The thickness of the face is specified as an input, so that volume is calculated exactly, which will result in accurate calculation of the mass and thermal capacity. Flanges are modeled as conduction coupling between two sides.

### 3.3.2 Solar Panels

Solar panels are present on four faces of the satellite. Three solar panels present on leading, lagging and Sunside faces of the satellite have a length of 260 mm and a width of 219 mm. The other solar panel present on the zenith surface has a length of 260 mm and a width of 164 mm. A distance of 12 mm must be kept between the solar panel and the satellite body. This space will be used for applying the Multilayer insulation (MLI). The solar panel is also modeled as a shell element with a thickness of 3 mm. It is attached to the satellite faces by a steel screw of 3 mm diameter and GFRP washers at the four corner points of the solar panels. Therefore a conduction coupling condition is applied between the solar panels and the satellite faces at these points.

### 3.3.3 Multilayer Insulation

The empty space between the solar panels and the satellite face is filled with multilayer insulation (MLI). MLI is modeled as a shell element with a thickness of 10 mm covering the entire area of the satellite sides. Here, a conduction coupling is applied between the entire face of the satellite side with entire face of the MLI. Conduction coupling is not applied between solar panel and MLI, as the MLI is not in contact with the solar panels. here. Nevertheless, a radiation coupling is applied between MLI and solar panel.

### 3.3.4 Battery Box

The battery box present in the Nadir side consists of a hollow box without bottom(along nadir side) with a dimension of 80 x 74 x 42 mm and thickness of 2 mm. The box contains six batteries. It is modeled as shell element of thickness 2 mm. These five faces were not connected so, they were stitched together along edges for purpose of conduction. Battery Box is attached using stub which has a hole, through which screw is inserted. GFRP Washers of 3 mm are present between Nadir side and stubs, which is modeled as conduction coupling. Along with battery box, stubs attached to it is also made in cad model. Mid surfaces of stubs were created, which are parallel to Nadir side. Mid surface of stubs are stitched with Battery box along its edge. Then, conduction coupling between Stub and corresponding element of Nadir side connected by stubs is defined. Conduction through screw is ignored. Battery box will be covered by MLI on all of its five faces. For modeling purpose, mid surface of MLIs have been created and conduction coupling is defined between MLI and corresponding battery box face.

### 3.3.5 GPS

The GPS present in the zenith side consists of a hollow box with outer dimension of 125 x 55 x 40 mm. It's modeled as shell element of thickness 11.8 mm. In CAD model outer dimension has been kept same as physical model. Thickness of 11.8 mm has been decided using mass constraint. Though it's not a good approximation because it's considerably thick but, since we need rough idea of temperature range of GPS and to reduce the computational time, it was modeled as shell element. It is not in direct contact with zenith, but is attached to the zenith using screws inserted through aluminium stubs. These stubs are modeled as conduction coupling between GPS surface and zenith.

### 3.3.6 Magnetometer

The modeling of the magnetometer is similar to that of GPS. It has outer dimension of 107 mmX38 mmX22 mm. It is modeled as shell of 3.8 mm thickness. In CAD model outer dimension has been kept same as physical model. Thickness of 3.8 mm has been decided using mass constraint. It is not in direct contact with lagging side, but is attached to the lagging side using screws inserted through aluminium stubs. These stubs are modeled as conduction coupling between magnetometer and Lagging side.

### 3.3.7 Printed Circuit Boards (PCB)

There are total of six PCBs present namely, the downlink, beacon, uplink, power, OBC and the sun sensor board. These PCBs have a thickness of 1.65 mm. Power and obc board are of dimension 128 mmX128 mm and are connected to satellite body by stubs of cross section 10 mmX10 mm and lenght 15 mm. Beacon, uplink and downlink have dimension of 161 mmX51 mm and sun sensor board is of dimension 120 mmX76 mm. These boards are connected to satellite body by stubs of cross section are 10 mmX10 mm and lenght of 10 mm. These are attached to the satellite sides using screws inserted through stubs.

Stubs are modeled as thermal coupling between satellite side and pcbs while conduction through screws is neglected. The PCBs have electrical components that dissipate heat. Total heat dissipated by these components is applied as heat load on corresponding pcb. There are heat sinks on beacon, downlink and uplink boards. Their midsurface is created and thin shell property is defined.

### 3.3.8 Monopole

Three cylindrical monopoles are present on the antisunside face of the satellite. The monopole has a holder, which is placed on a square base, which is attached to antisunside using screws. It is modeled as long rod of rectangular cross section. Length and cross-section area is kept same as in actual design, length of cross section is kept in such a way that after creating mid surface of rectangular monopole, surface area of mid surface and curved surface area of cylindrical monopole in actual design are same. So that radiation to environment is correctly modeled.

### 3.3.9 Magnetorquer

There are three rectangular magnetorquers of 'c' cross section on Zenith, Sunside and Leading sides, one on each. In CAD model, they are approximated as of rectangular cross section. They are also modeled as midsurface with thin shell property as thickness of 8 mm. Thickness is decided by mass constraint.

## 3.4 Grid

The model has been meshed using a structured grid. Quad4 elements are used for meshing. Total 9359 elements are created after meshing the model.

## 3.5 Boundary conditions and Couplings

Boundary Conditions defines known thermal conditions in the model. The Thermal Boundary condition consist of a variety of heat loads and fluxes, fixed temperatures, and joule heating. Thermal coupling are applied to specify conductance between two dissimilar meshes or to specify conductance between two surfaces that are connected through screws or stubs. In this section, we explain in detail all the boundary conditions and the coupling applied in the model

### 3.5.1 Solar Fluxes

Orbital heating option is used to determine heat flux as function of time that will fall on each face of satellite. Satellite has a 22.30 sun synchronous orbit. After giving input parameters like altitude, eccentricity etc. heat flux can be received for all the faces of the

satellite. Solar flux was applied on respective faces and solar absorptivity of respective surfaces are defined.

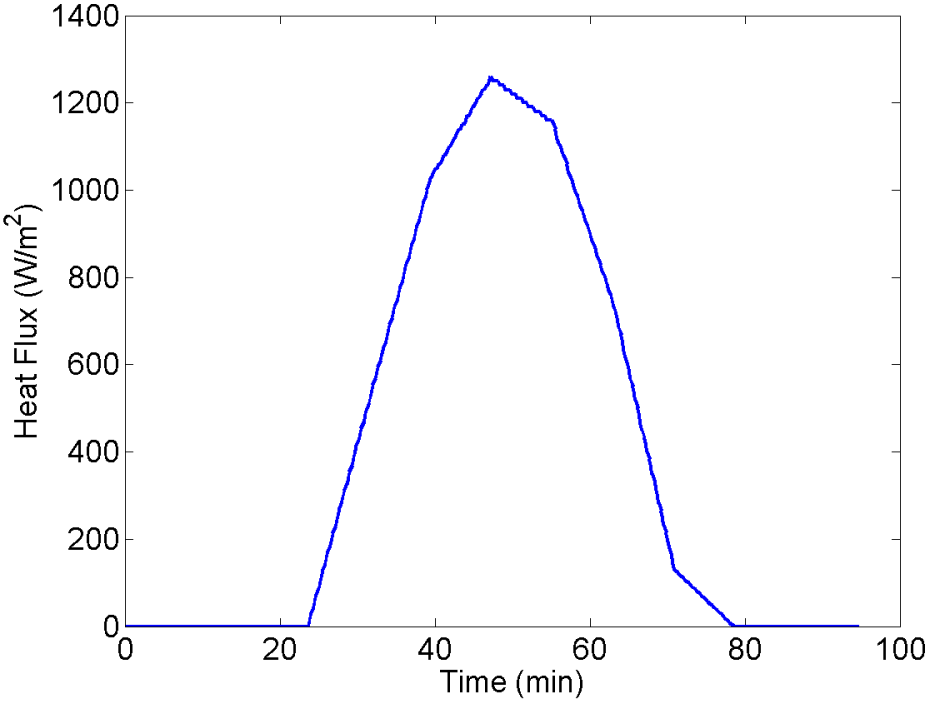


Figure 3.1: Solar Flux: Zenith

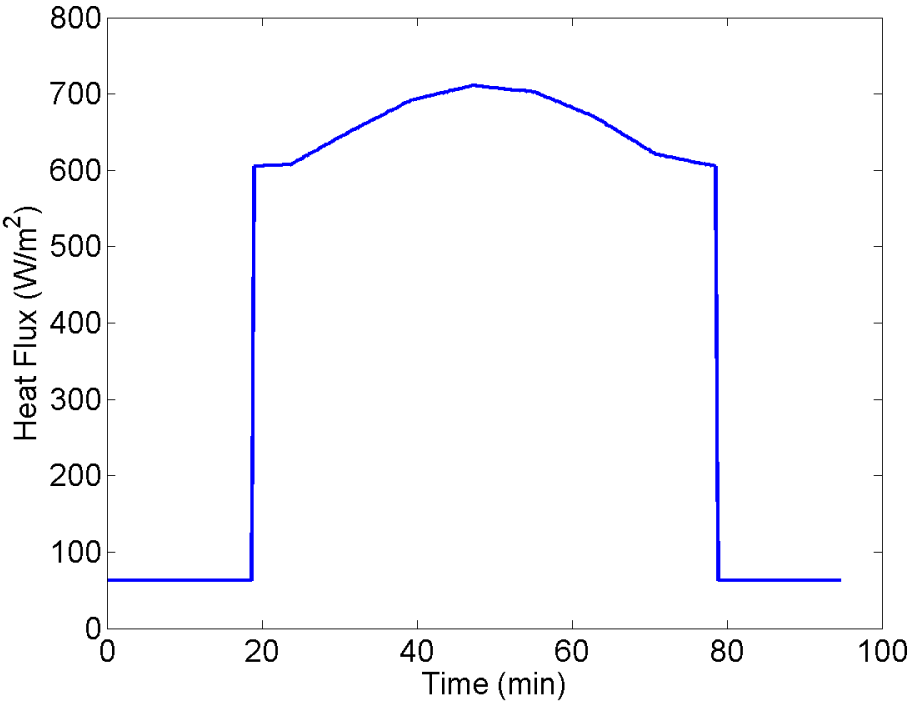


Figure 3.2: Solar Flux: Sunside

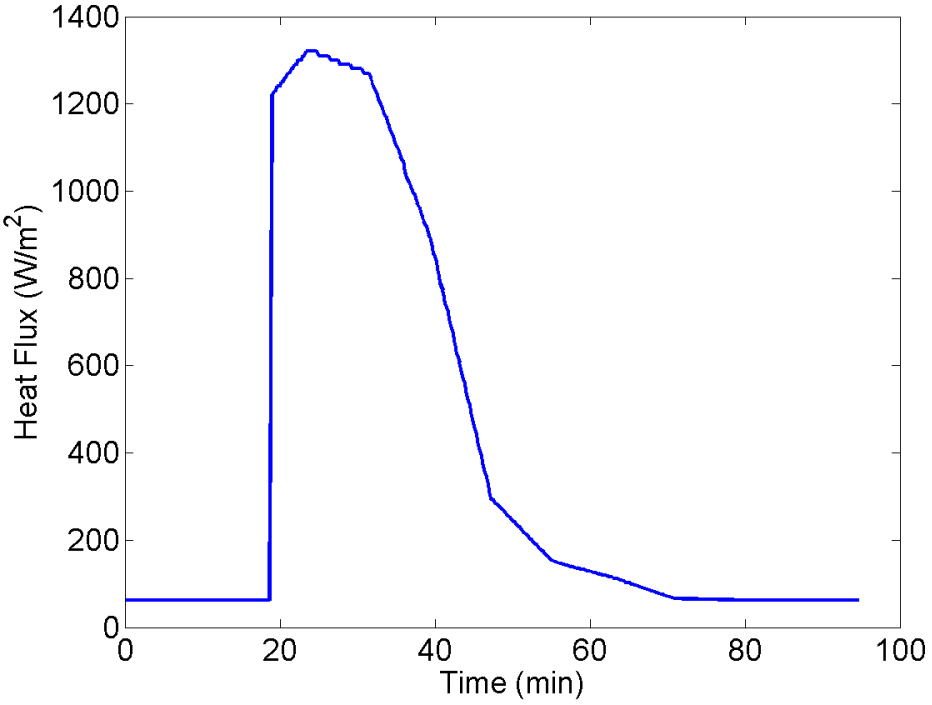


Figure 3.3: Solar Flux: Leading

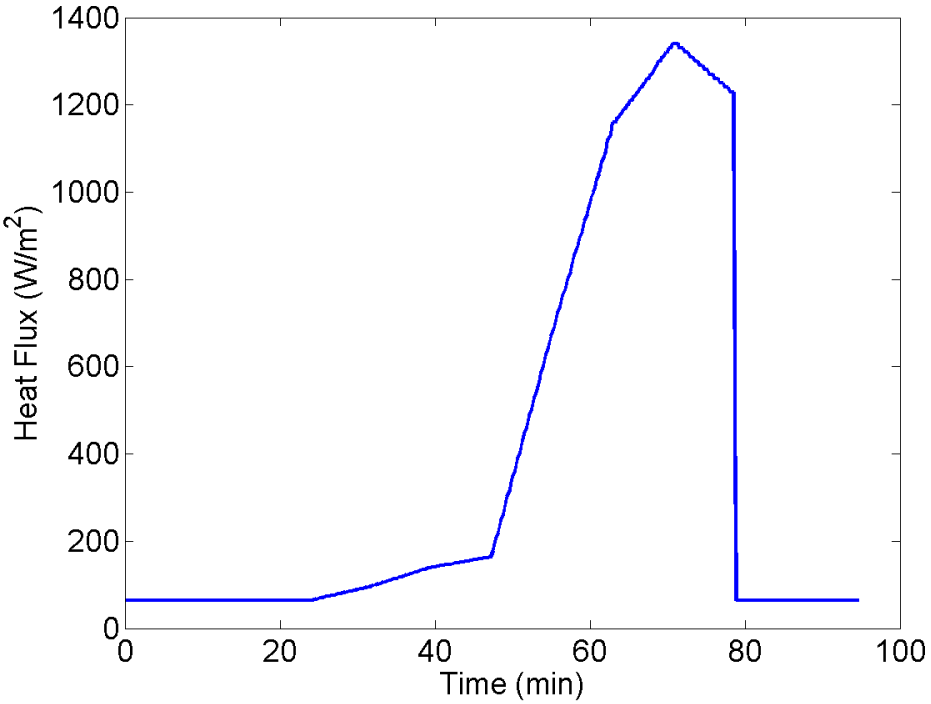


Figure 3.4: Solar Flux: Lagging

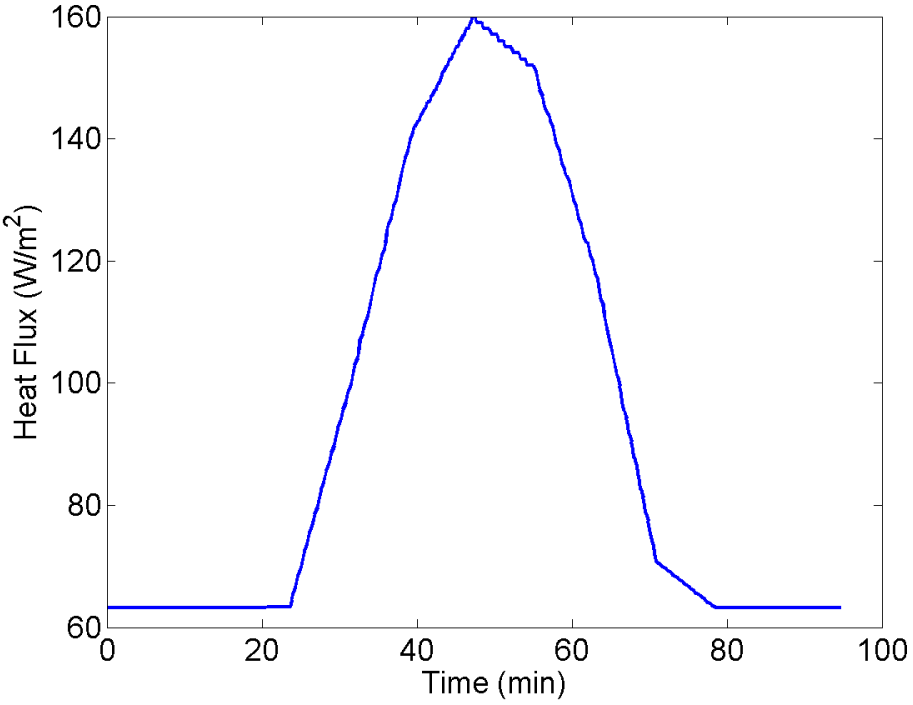


Figure 3.5: Solar Flux: Anti-Sunside

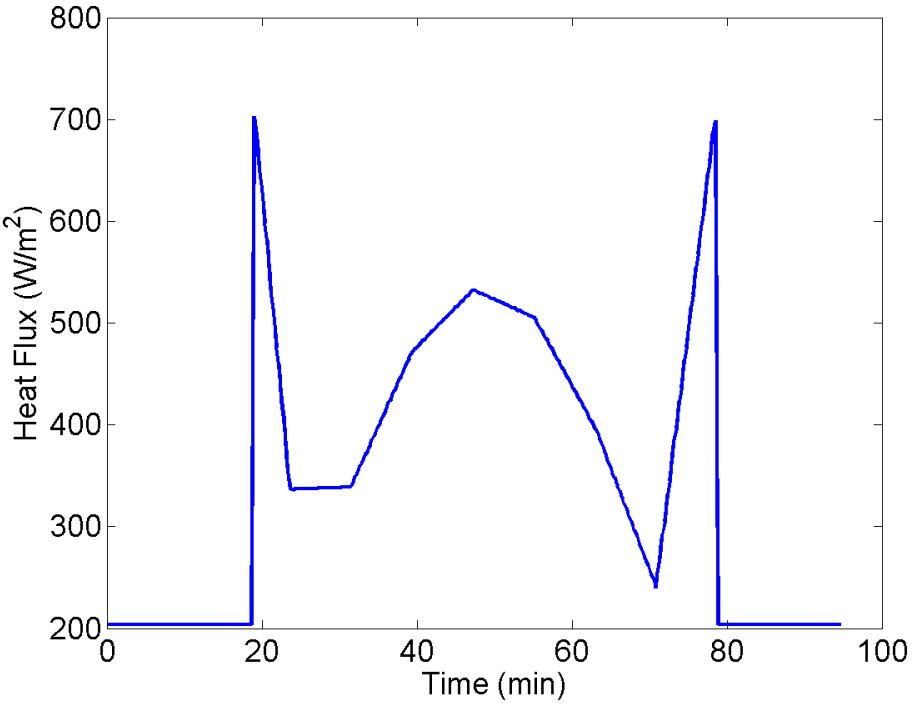


Figure 3.6: Solar Flux: Nadir

Source: NASTRAN Simulation

### 3.5.2 Heat dissipation from PCBs

Electrical components on the PCBs are major source of heat dissipation in the satellite. The electrical components on the PCB generate heat. We have heat dissipation data for all the PCBs which was applied as heat load on respective PCBs. Heat sinks are used on Downlink and Beacon boards for power amplifier and LNA on Uplink board as their heat dissipation is relatively more. Heat sinks are designed in CAD model and its mid surface is created in NASTRAN for analysis. Heat generated in Power amplifiers are applied as heat load on Heat sinks. Heat sinks are connected to stubs by screws through PCB. Stub and screw is modeled as total conductance between heat sink and satellite side. Heat sink is also connected to PCB by screws which are modeled as total conductance between heat sink and PCB. Thermal filler material is applied between heat sink and PCB for proper contact between them. TPS on power board are not modeled individually even though their heat dissipation value is more than 0.1 W due lack of its thermal property data. Instead, total heat dissipation is given on entire power board just to ensure that all the heat loads are taken into account. heat table-:

| PCB | Heat dissipated(W) |
|---|---|
| OBC | 0.1425 |
| Beacon | 0.0425 |
| Beacon Power Amplifier | 1.7 |
| Downlink | 0.0836 |
| Sun Board | 0.025295 |
| Uplink | 0.14917 |
| LNA | 0.055 |
| Magnetorquer | 0.2924 |
| GPS | 2 |
| Magnetometer | 1.28 |
| Battery Box | 0.08 |

Table 3.2: Heat Loads: In-Orbit

**Variable Heat Loads:**

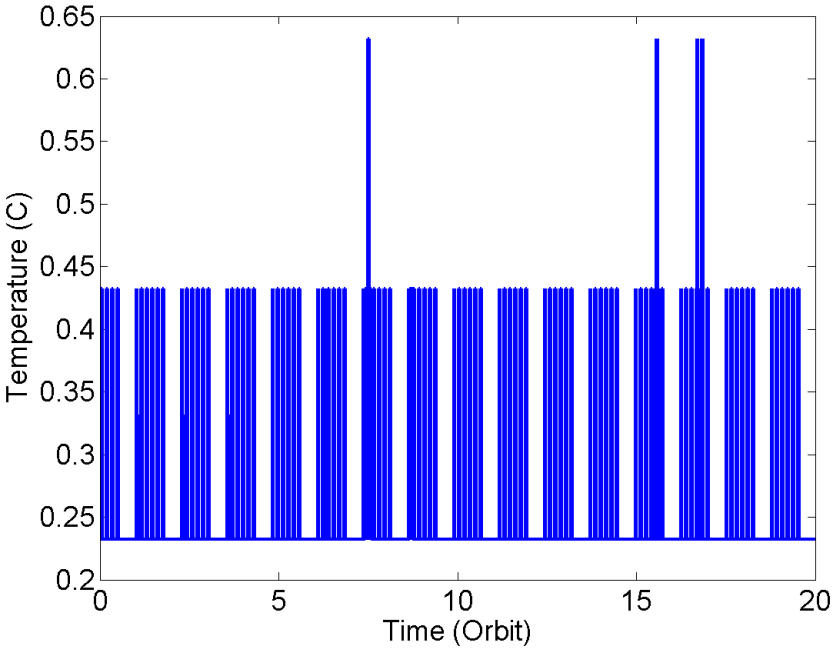


Figure 3.7: In-Orbit Heat Load: Power Board

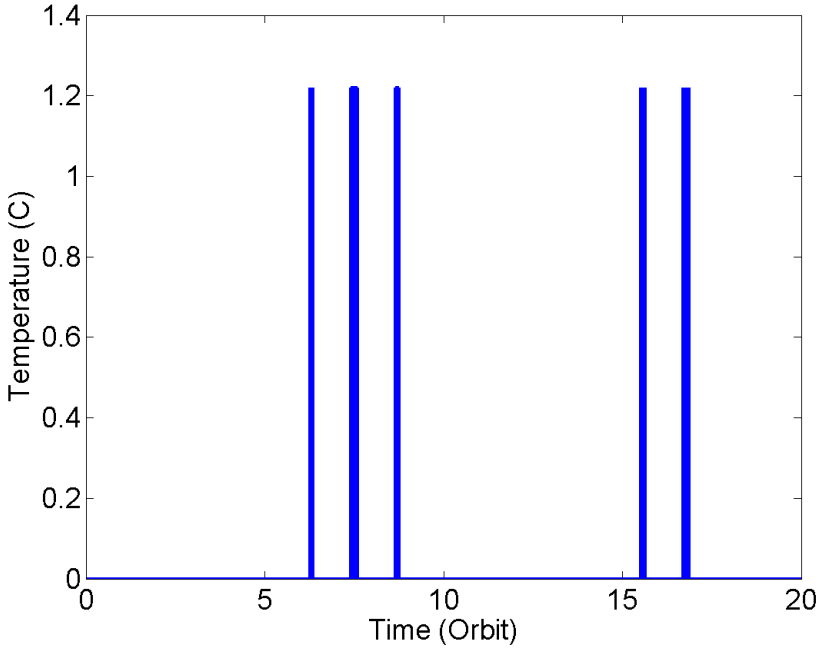


Figure 3.8: In-Orbit Heat Load: Power Amplifier on Downlink

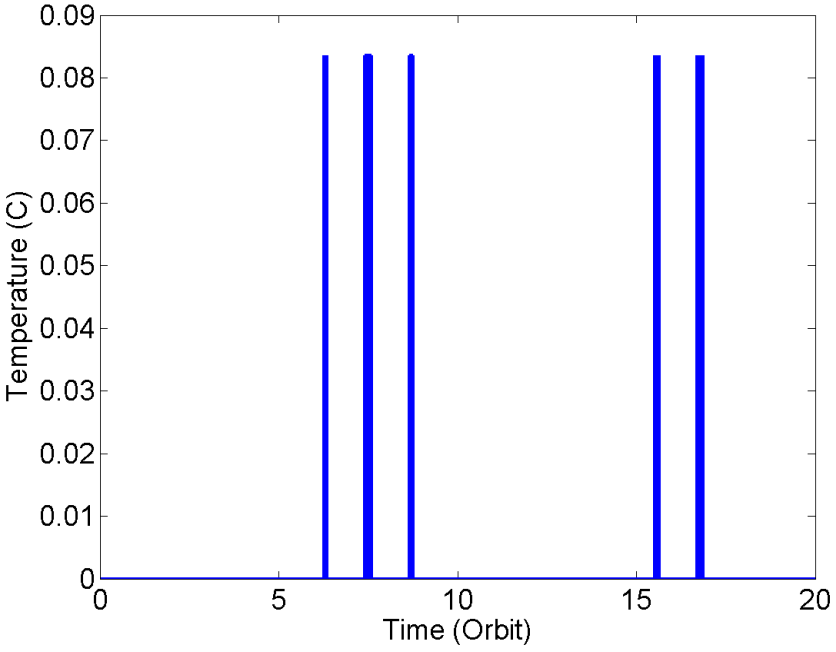


Figure 3.9: In-Orbit Heat Load: Downlink Board

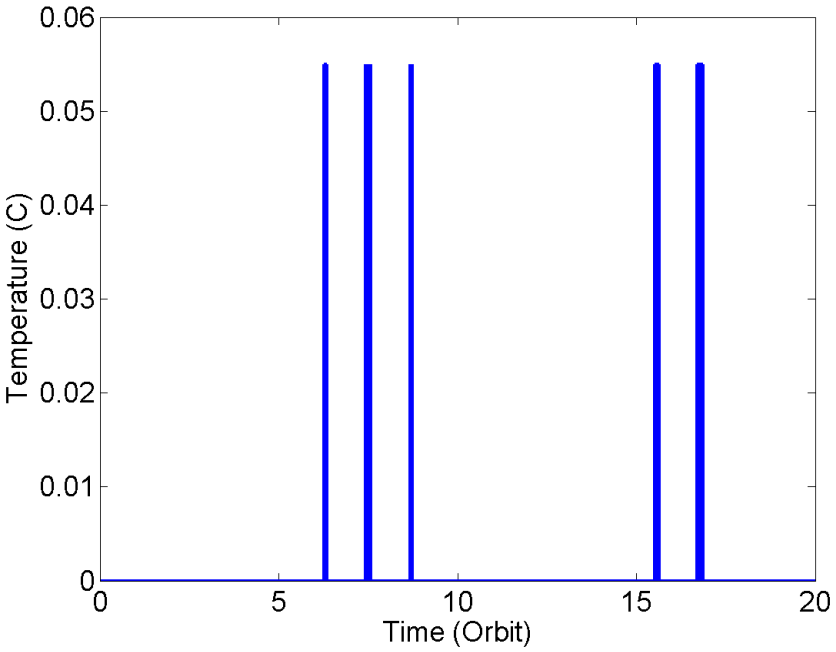


Figure 3.10: In-Orbit Heat Load: LNA on Uplink

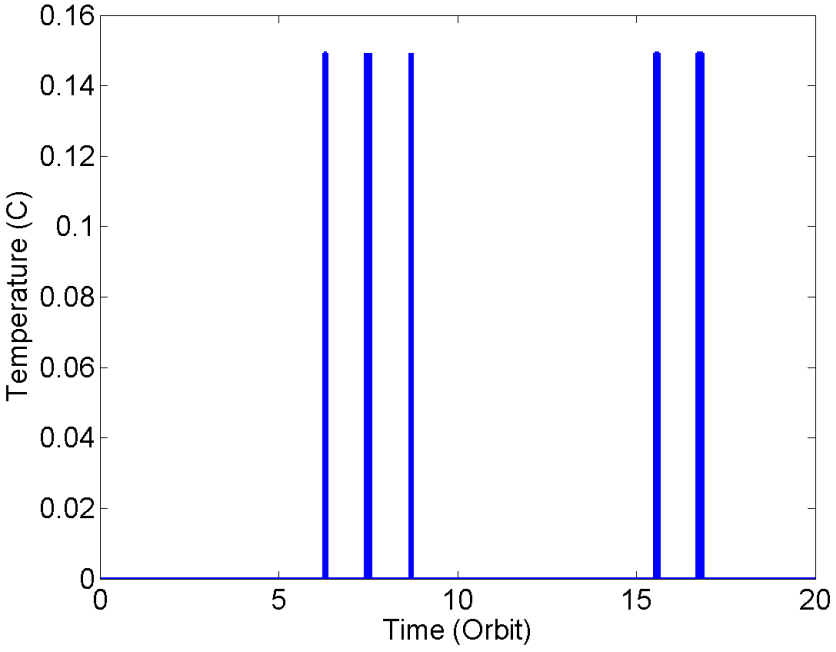


Figure 3.11: In-Orbit Heat Load: Uplink

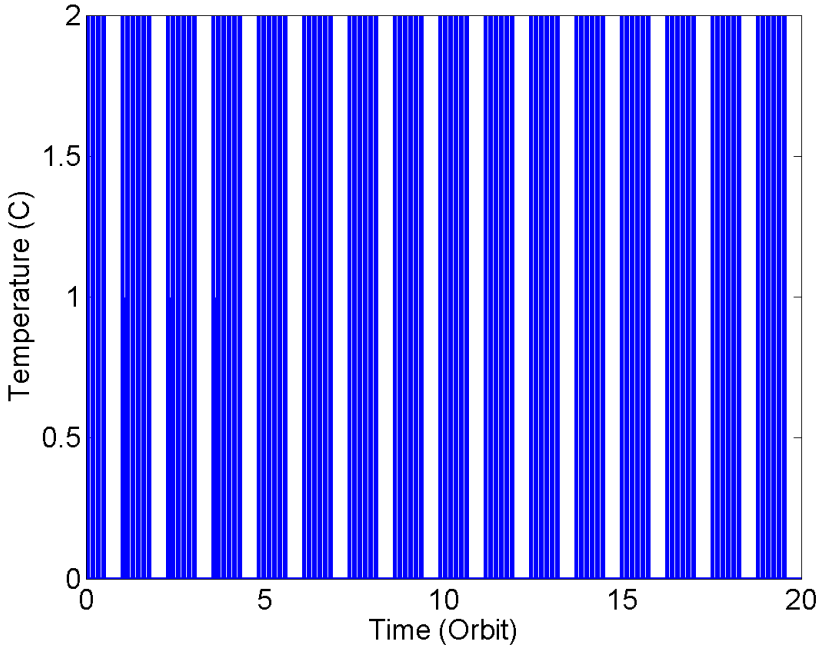


Figure 3.12: In-Orbit Heat Load:GPS Box

### 3.5.3 Thermal coupling between solar panel and satellite sides

The solar panels are attached to the satellite sides using screws of 3mm diameter. The solar panels are at a distance of 12 mm from the satellite sides. The conduction through the screws is modeled by coupling condition.We apply conductive coupling which creates conductance G = (K x A) / L from the primary elements to the nearest secondary elements, where L is the distance to the secondary element along the primary element's surface normal, which is 12 mm in this case. The element mesh of the satellite sides should be prepared such that the element size has the approximate area of the screw. Then the element, that holds the approximate location of the screw should be selected as the primary element and the element in solar panel, nearest to the screw should be selected as the secondary element. The area A is calculated from the area of the primary element and conductivity, K of the steel is specified.

### 3.5.4 Radiation coupling between MLI and solar panels

It creates radiative conductance between the primary and secondary elements. The magnitude of conductance is equal to: $\sigma\cdot$ GBVF $\cdot\ \varepsilon_1\ \cdot$ $A_1$ $(T_1^2+ T_2^2)(T_1 + T_2)$ is the Stefan-Boltzmannconstant.
GBVF is the specified gray body view factor,
$\varepsilon_1$ is the emissivity of the primary elements,
$A_1$ is the area of the primary elements,
$T_1$ is the absolute temperature of the primary elements, and

$T_2$ is the absolute temperature of the secondary elements.
The gray body view factor is the net amount of radiation emitted by the primary elements and absorbed by the secondary elements including all intermediate reflections. The separate element defined on reverse side of the solar panel for the purpose of radiation is selected as the primary element. The element on the front side of the MLI is selected as the secondary element. View factor is calculated between MLI and Solar panels using MATLAB code.

### 3.5.5 Thermal coupling between MLI and satellite sides

Conduction between MLI and side panels is defined as 'Total Conductance' calculated using heat transfer co-efficient (h) = 0.1 W/($m^2$ K)

### 3.5.6 Conduction Coupling between PCB and satellite sides

The PCB is attached to the satellite sides using screws inserted through the stubs. Stubs(10mmx10mm) has more area than that of screws(7.065 $mm^2$) as well as conductivity(stubs - 155 W/m-K, screws - 16.2 W/m-K). So, most of the heat transfer will take place through stubs. Total conductance is defined between pcb and satellite body. The elements having the approximate location and area of the stubs at the satellite sides are specified as the primary element and the corresponding elements in the PCB are specified as the secondary elements. Conduction through stubs is modeled by total conductance while conductance through screws is neglected.

## 3.6 Internal radiation

All the surfaces inside the satellite radiate among each other due to the virtue of its temperature. Internal radiation is modeled by defining 'Enclosure Radiation' in NASTRAN. It calculates view factor and takes all the internal radiation into account.

## 3.7 OSR

OSR has been modeled as radiation to environment with emissivity of 0.78 on antisunside. It has been applied on entire Anti-sunside face of the satellite.

## 3.8 Transient Analysis

Thermal analysis has been done using NX space system thermal solver. Total 9101 elements and 10000 modes were created after 2-D meshing of entire model. For any transient simulation, we must define the time span for the solution. In addition, we should also specify the Time Step, which is the time mesh for the solution. A smaller time step will

give more accurate results at a cost of increased computation time. A time span of 20 orbits is specified for simulation. Time step of 30 second is used.

# Chapter 4

# In-orbit Results

The simulations are carried out based on the modeling described above. After the first round of simulations, temperatures on the various parts of the satellites were observed. After analyzing the temperature of the various parts, which parts require thermal treatment was decided. Thus, on the basis of the temperatures, we decided the thermal design that will be applied on the flight model. All the decisions related to thermal design have been stated below

- All the packages (including battery) which are mounted inside the spacecraft will be covered with black paint to maintain uniform temperature.
- All spacecraft panels will be black anodized from inside and covered with MLI blanket (8 layers) from outside on four sides which have solar panels on it.
- High dissipated chips (which dissipate 1W) will be placed on the Telemetry and Beacon PCB using thermal filler materials along with heat sink.
- All solar panels will be isolated from the spacecraft panels conductively and radiatively.
- All solar panels back side will be covered with low emittance tape (e = 0.05).
- GFRP Washer of thickness 3 mm is used between nadir side and battery box to reduce swirling of battery box temperature.
- Payload antenna consists of one holder and one monopole. Total three antennas are mounted on the spacecraft anti sun side panel.

## 4.1 Max and Min temperatures of different components

Following are the results of simulation done for 20 orbits for altitude of 500 km. Temperature has been given after initial fluctuation in temperature has stabilized, starting from initial temperature of $20^0$C.

| SI. No. | Components | Min ($^0$C) | Max ($^0$C) |
|---|---|---|---|
| 1 | Zenith Solar Panel | -49.9 | 65.3 |
| 2 | Sunside Solar Panel | -43.0 | 32.5 |
| 3 | Leading Solar Panel | -95.7 | -18.6 |
| 4 | Lagging Solar Panel | -92.8 | -8.6 |
| 5 | Zenith MLI | -47.0 | 64.7 |
| 6 | Sunside MLI | -40.8 | 32.3 |
| 7 | Leading MLI | -88.5 | -46.8 |
| 8 | Lagging MLI | -86.6 | -40.0 |
| 9 | Zenith Side Panel | 16.9 | 18.6 |
| 10 | Sunside Side Panel | 19.7 | 21.9 |
| 11 | Leading Side Panel | 18.2 | 20.2 |
| 12 | Lagging Side Panel | 19.0 | 21.1 |
| 13 | Nadir Side Panel | 23.8 | 29.3 |
| 14 | Anti-Sunside Side Panel | 13.4 | 15.3 |
| 15 | Power Board | 20.6 | 23.2 |
| 16 | OBC Board | 19.2 | 20.9 |
| 17 | ADC Board | 18.8 | 20.4 |
| 18 | Uplink Board | 19.4 | 21.7 |
| 19 | Downlink Board | 17.4 | 19.9 |
| 20 | Beacon Board | 18.0 | 19.8 |
| 21 | LNA on Uplink Board | 17.6 | 19.7 |
| 22 | Power Amplifier on Downlink Board | 13.8 | 19.4 |
| 23 | Power Amplifier on Beacon Board | 22.5 | 24.2 |
| 24 | Uplink Board below LNA | 17.6 | 19.7 |
| 25 | Beacon Board below Heat Sink | 22.3 | 24.0 |
| 26 | downlink Board below Heat Sink | 13.8 | 19.3 |
| 27 | Battery Box | 22.4 | 24.2 |
| 28 | GPS | 16.6 | 18.3 |
| 29 | Magnetometer | 20.2 | 22.3 |
| 30 | Magnetorquer on Zenith | 17.7 | 19.6 |
| 31 | Magnetorquer on Sunside | 18.8 | 20.9 |
| 32 | Magnetorquer on Leading | 18.9 | 21.1 |
| 33 | Monopoles | 12.3 | 13.8 |

Table 4.1: In-Orbit Temperature: 500 km

## 4.2 Inferences

- Solar panels have high temperature fluctuations due to presence of the highly fluctuating solar flux incident on them.
- Exposed part of MLI on zenith side has higher temperature than MLI on other sides

because it faces direct solar radiation.

- Exposed part of MLI on zenith side has its maximum temperature greater than solar panel on the same side because solar panel is connected with side panel through screws (conductivity=16.2 W/m-K) for conduction purpose. Whereas, though MLI is in contact with side panel, its conductivity (0.05 W/m-K) is negligible. Also, emissivity of MLI (e = 0.45) is less than that of solar panel (e = 0.85).
- Solar panels have been isolated from the satellite sides both conductively and radiatively, so that the fluctuation in solar panels does not get reflected in the satellite body.
- Very less temperature variation ($\sim$ 6 $^0$C) for internal components including PCBs is observed.
- Satellite body temperature has less variation over the orbit.
- Temperature of electrical components and battery box is within the range of operating temperature.

So, it has been concluded that all components are within their required temperature range.

**Screenshots from simulations:**

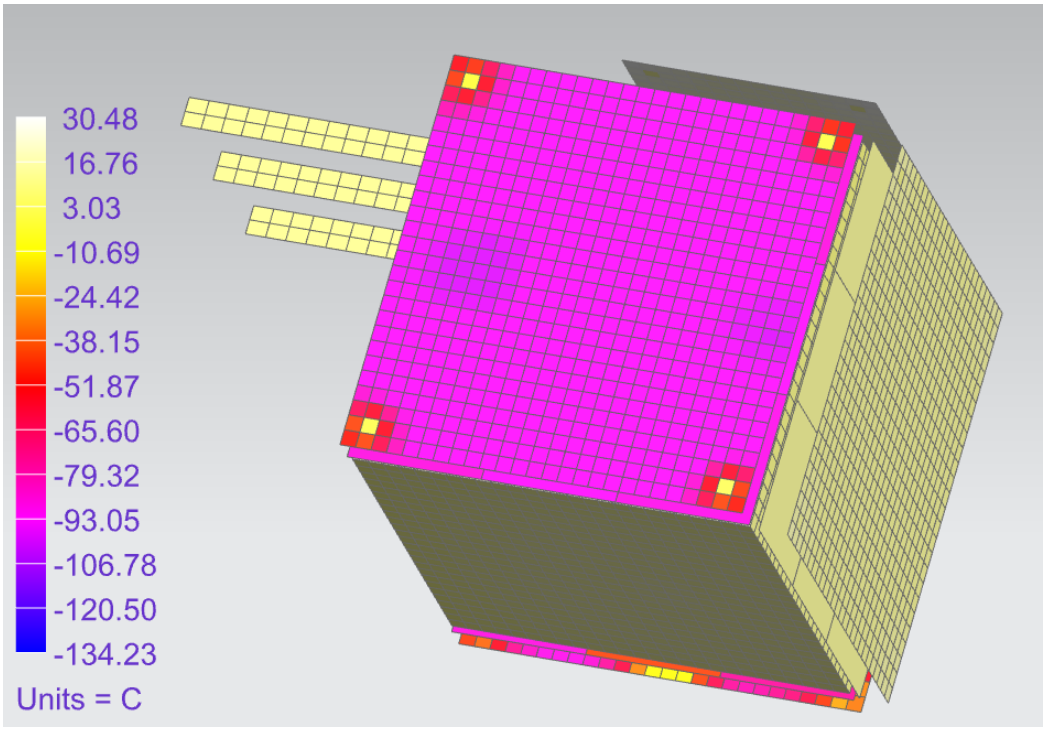


Figure 4.1: Solar panel and monopole temperature after 20 orbits for altitude: 500km

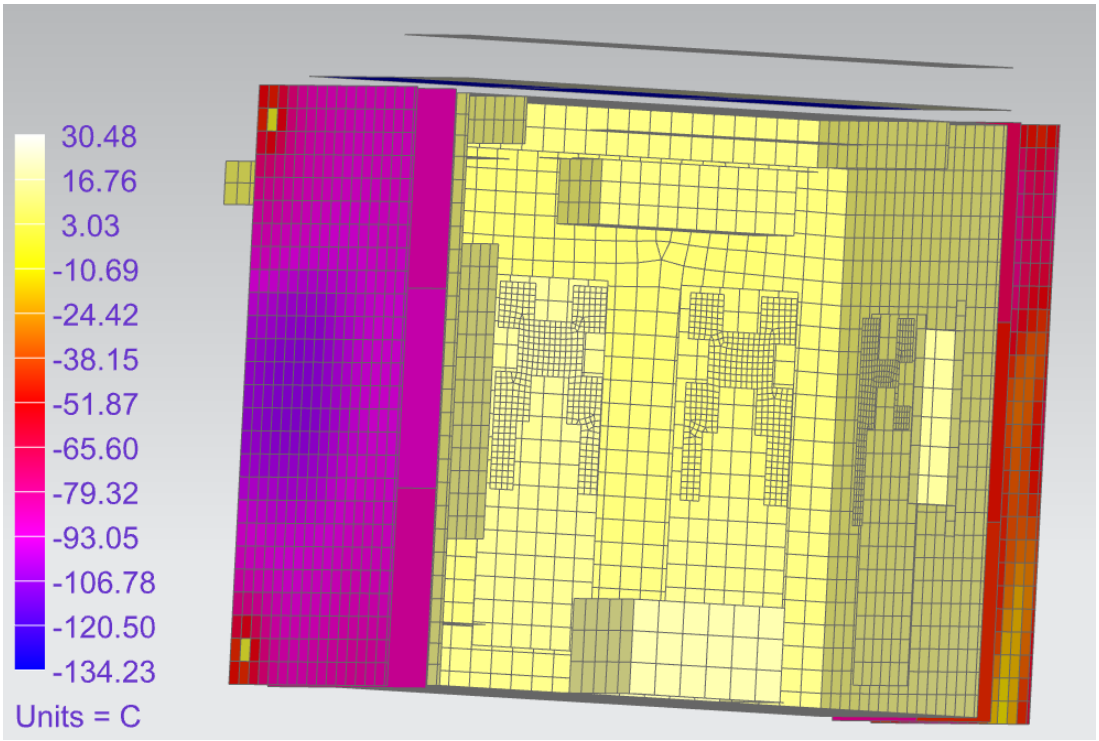


Figure 4.2: Solar panel and monopole temperature after 20 orbits for altitude: 500km

## 4.3 Temperature Plots for important components

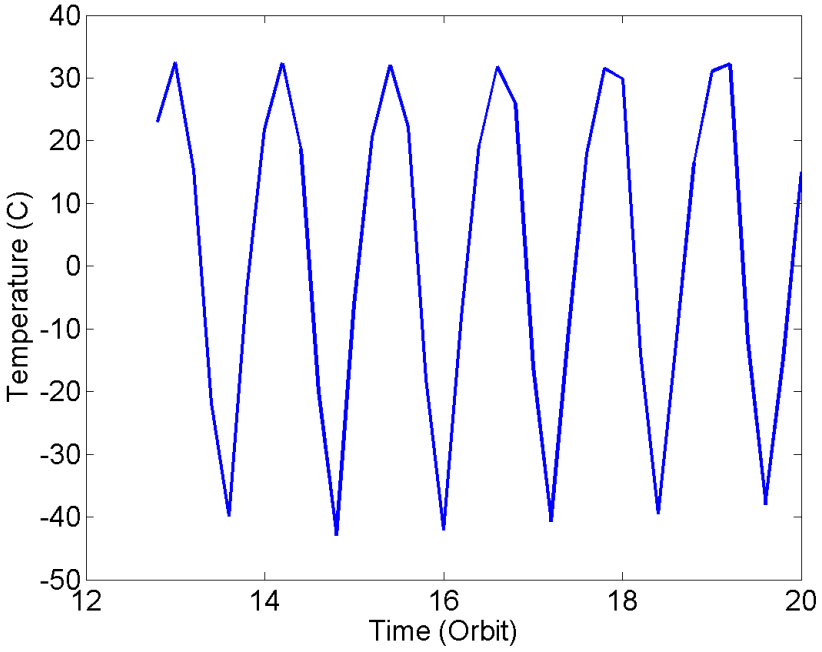


Figure 4.3: Temperature variation: solar Panel

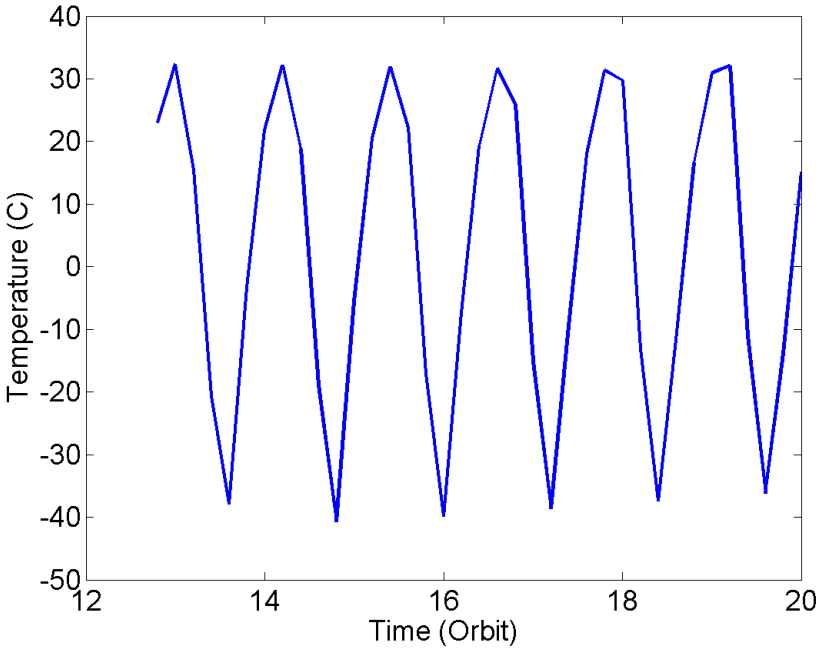


Figure 4.4: Temperature variation: MLI

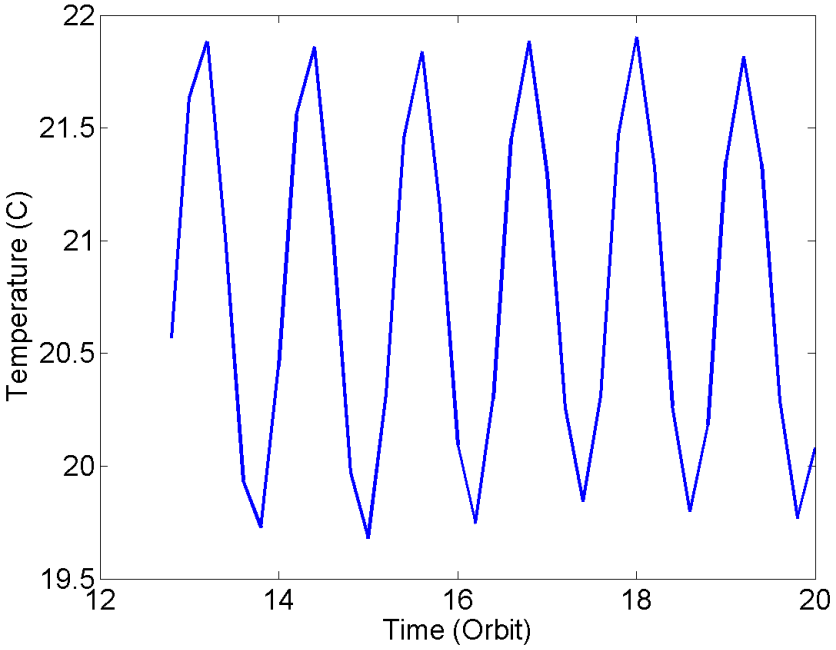


Figure 4.5: Temperature variation: Side Panel

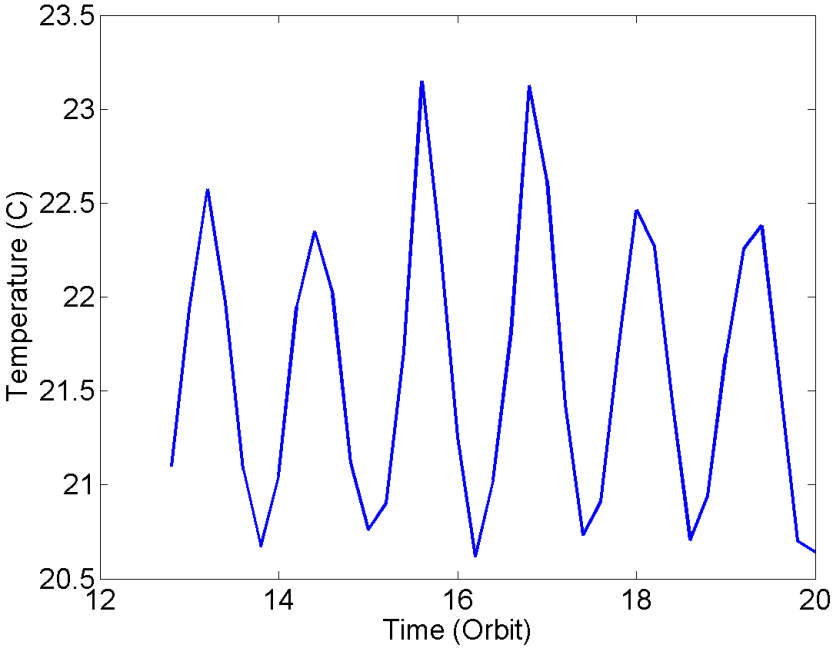


Figure 4.6: Temperature variation: Power Board

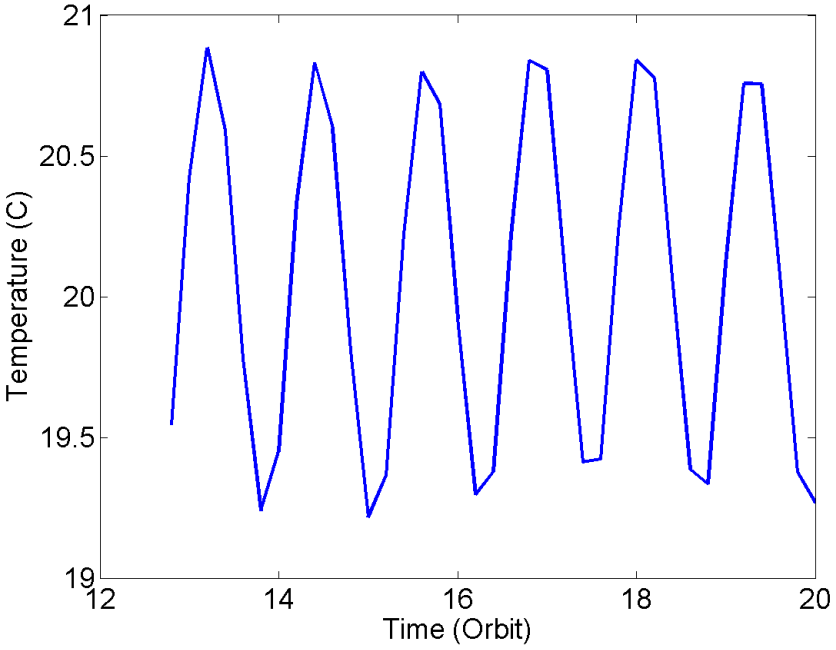


Figure 4.7: Temperature variation: OBC Board

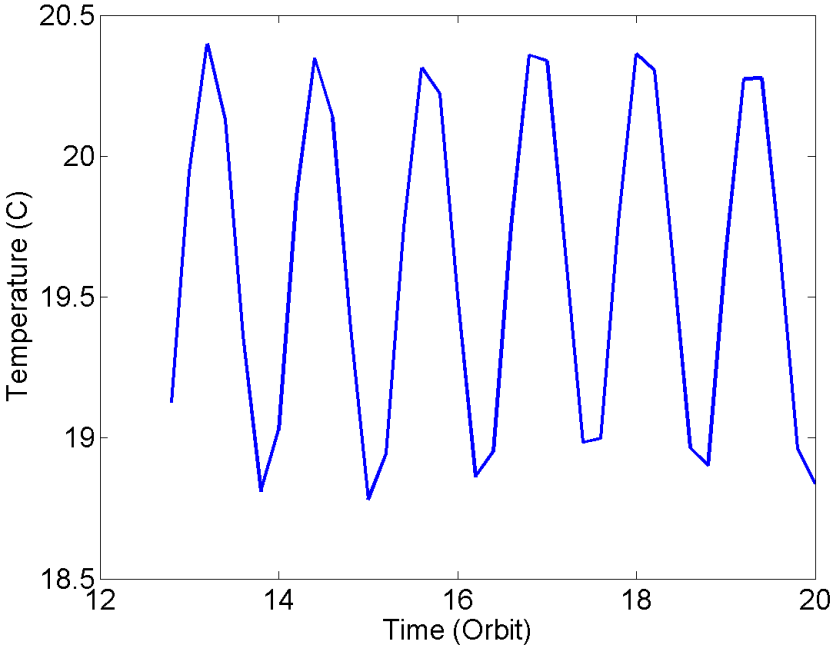


Figure 4.8: Temperature variation: Sunsensor Board

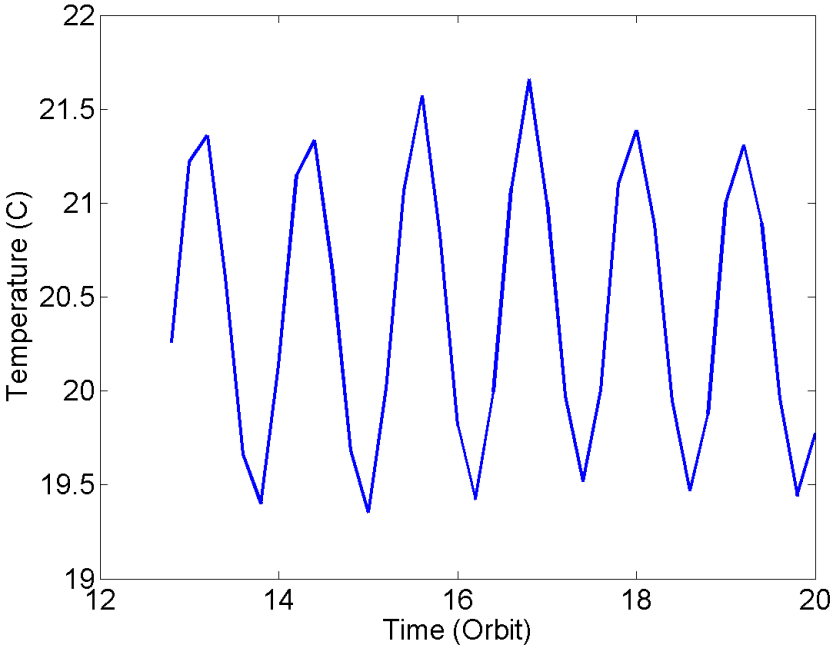


Figure 4.9: Temperature variation: Uplink Board

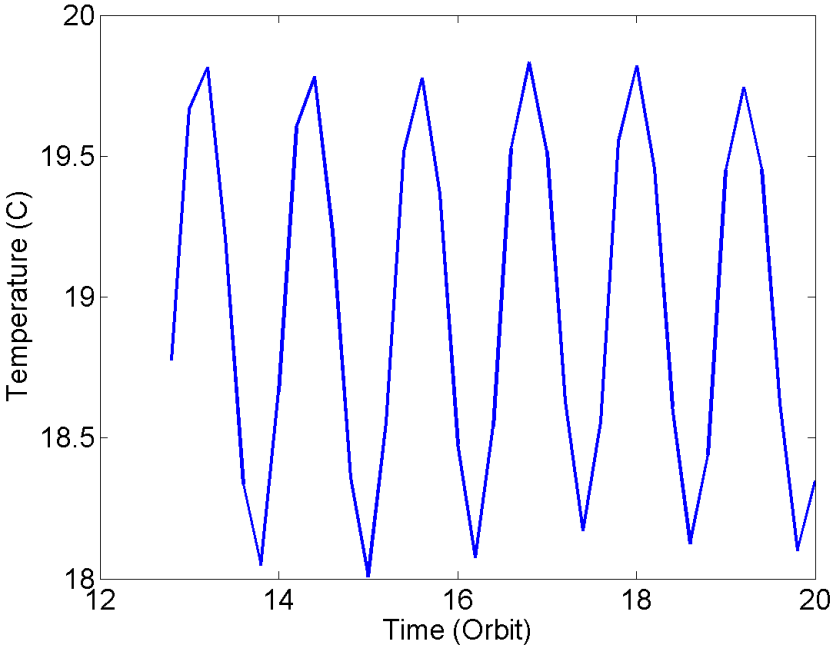


Figure 4.10: Temperature variation: Beacon Board

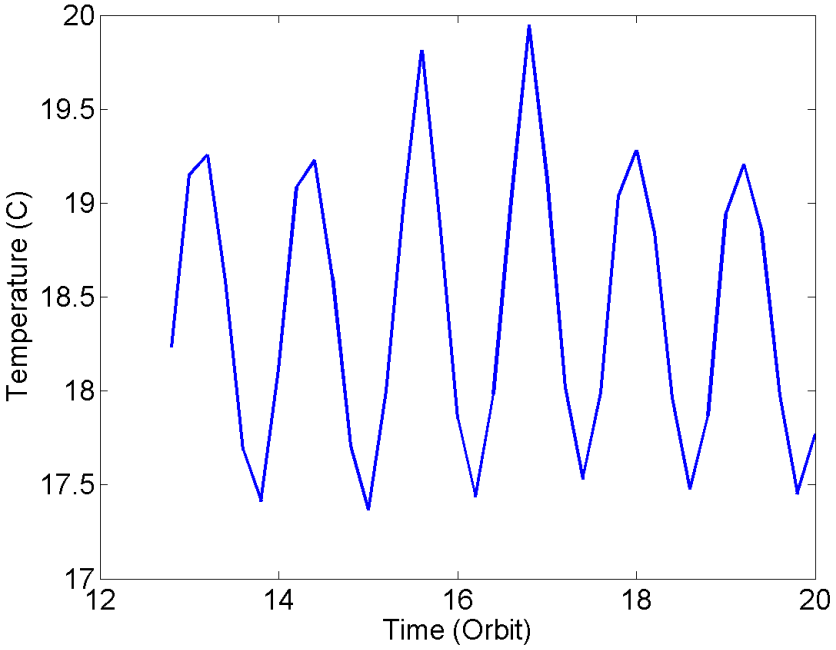


Figure 4.11: Temperature variation: Downlink Board

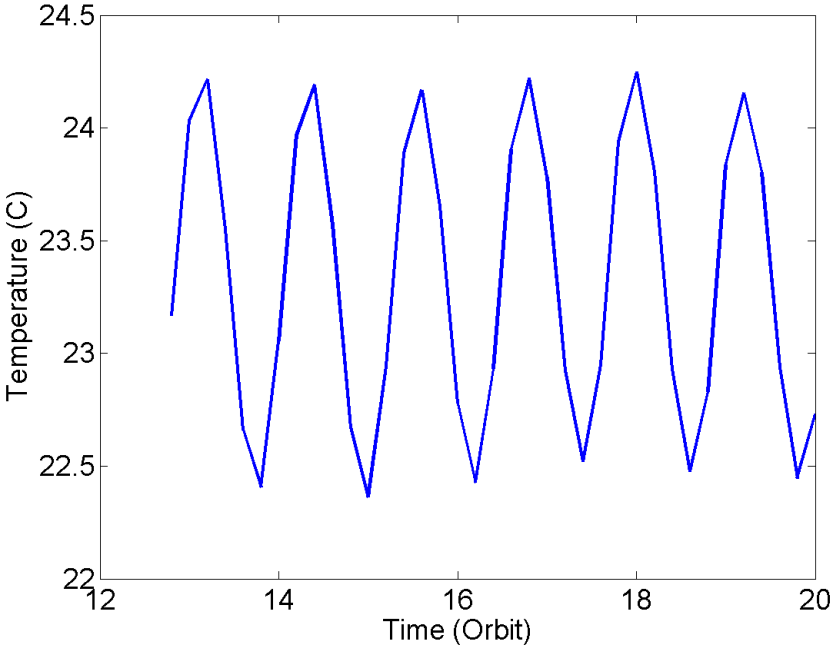


Figure 4.12: Temperature variation: Battery Box

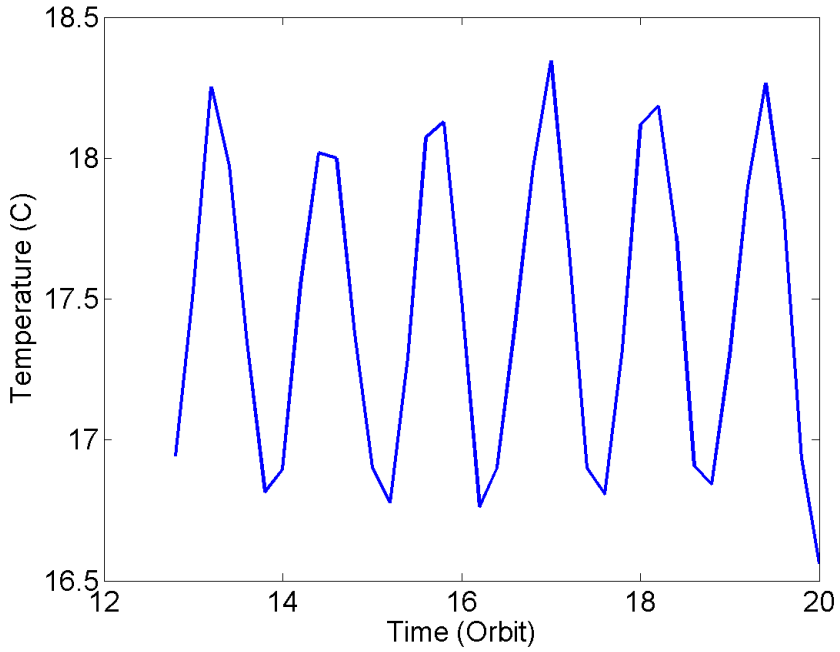


Figure 4.13: Temperature variation: GPS Box

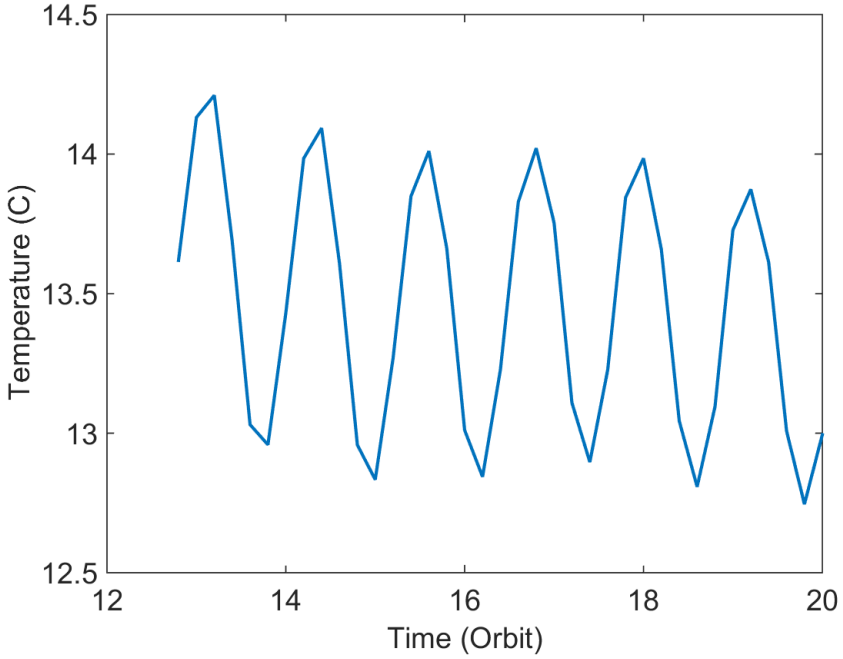


Figure 4.14: Temperature variation: Magnetometer

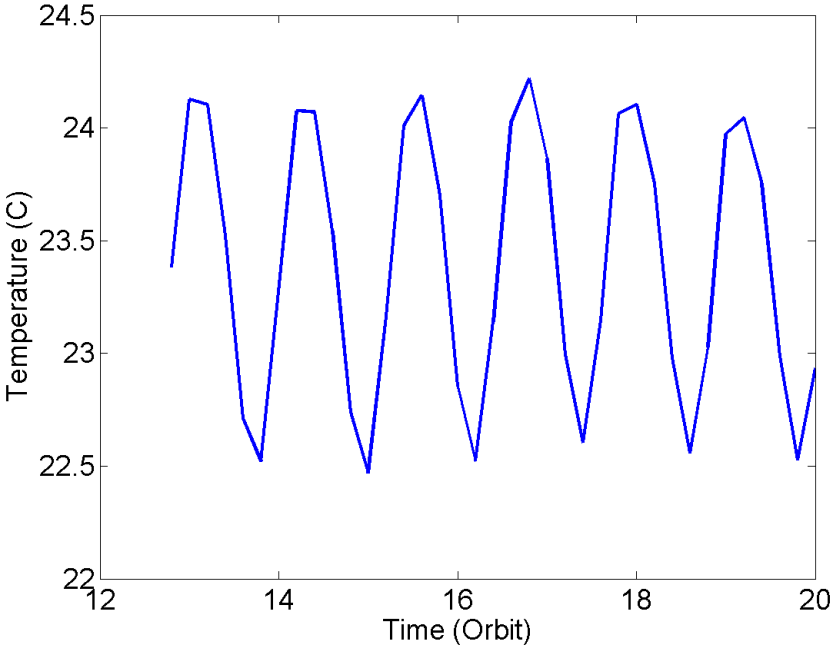


Figure 4.15: Temperature variation: Power Amplifier on Beacon Board

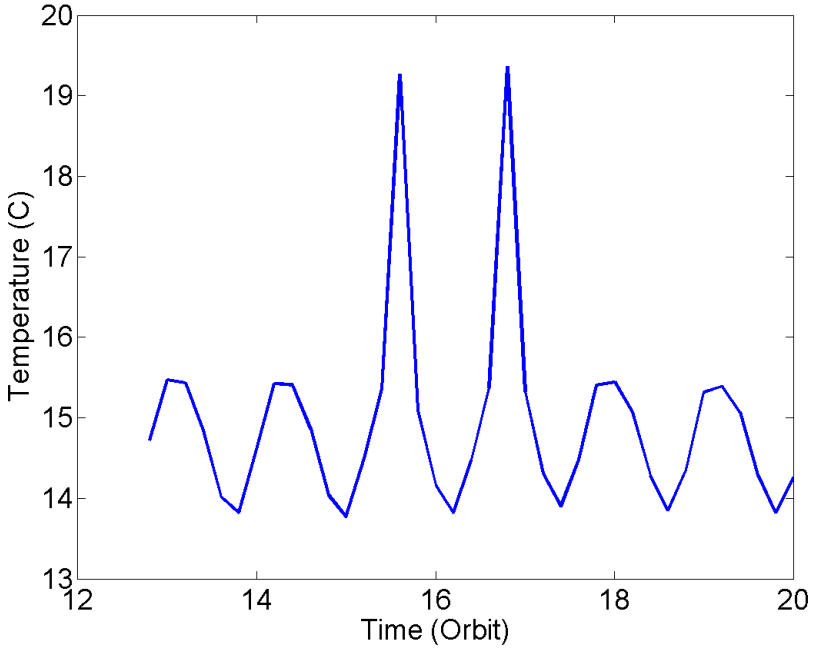


Figure 4.16: Temperature variation: Power Amplifier on Downlink Board

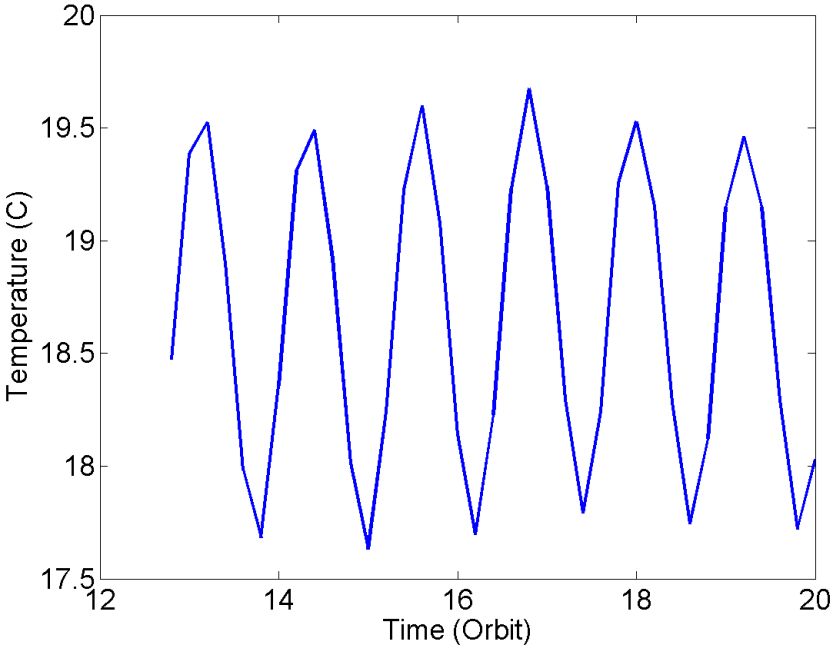


Figure 4.17: Temperature variation: LNA on Uplink Board

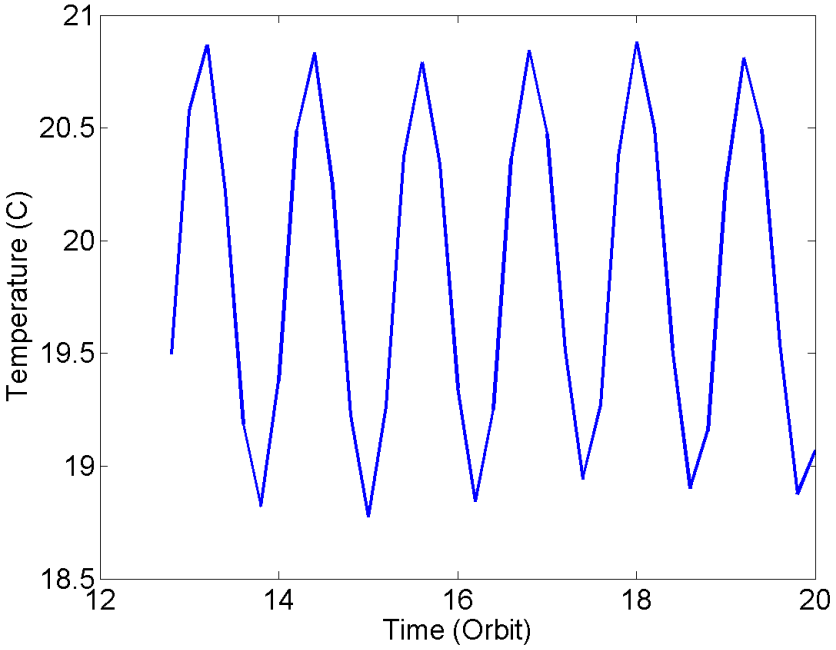


Figure 4.18: Temperature variation: Sunside Magnetorquer

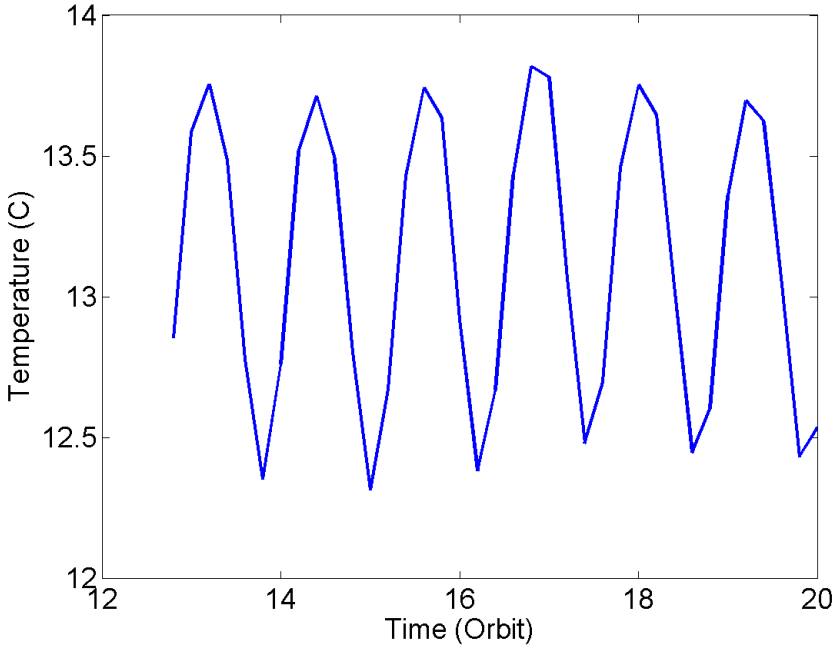


Figure 4.19: Temperature variation: Monopoles

# Chapter 5

# Thermovac Simulation

For thermovac testing time varying ambient temperature has been used. Two types of ambient temperature profile has been used which are given below. **Ambient temperature profile of soak duration 3 hrs each**

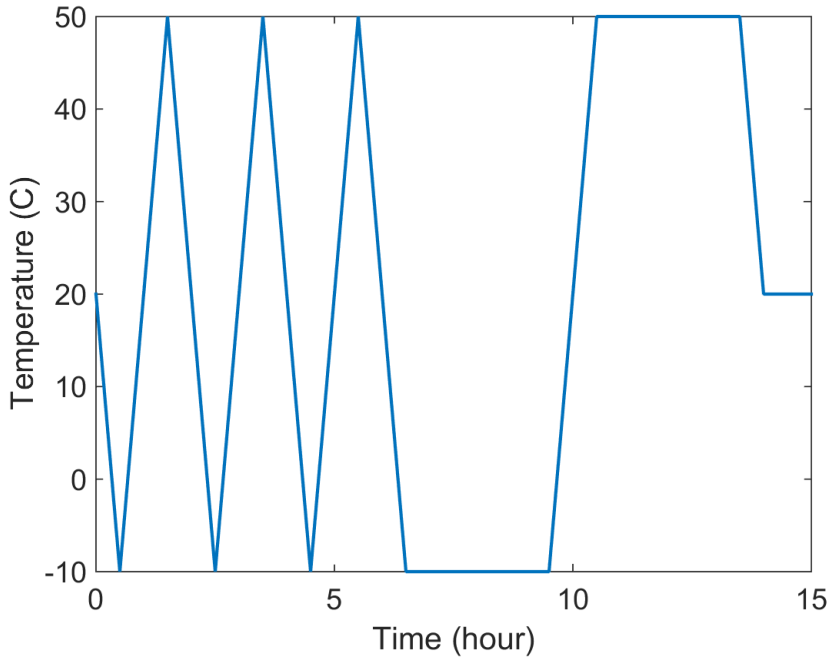


Figure 5.1: Thermovac Profile: Soak duration of 3 hrs each

In transient cycle slope is $1^0$/min. After third cycle when ambient temperature reaches to -$10^0$C after 6.5 hours, it is maintained at this value till another 3 hours for cold soak. Then, temperature is increased to $50^0$C with slope of $1^0$/min and then kept constant at this value for another 3 hours for hot soak.

**Ambient temperature profile of soak duration 4 hrs each**

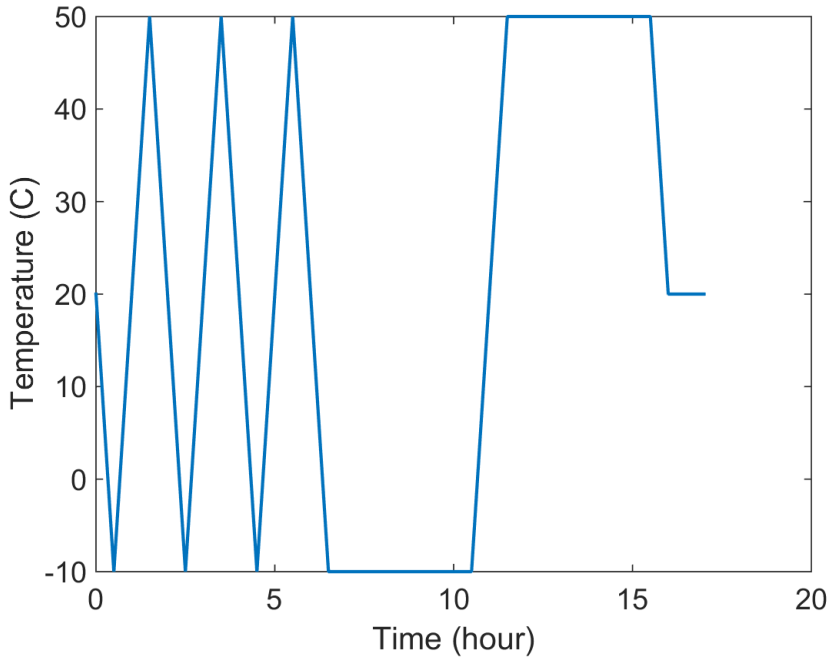


Figure 5.2: Thermovac Profile: Soak duration of 4 hrs each

In transient cycle slope is $1^0$/min. After third cycle when ambient temperature reaches to -$10^0$C after 6.5 hours, it is maintained at this value till another 4 hours for cold soak. Then, temperature is increased to $50^0$C with slope of $1^0$/min and then kept constant at this value for another 4 hours for hot soak.

## 5.1 Analysis

Thermal modeling of satellite for thermovac has been done in similar way as in-orbit modeling. All the thermal and radiation couplings are defined like it is done in in-orbit case. There are few changes in heat loads. Solar flux is not applied. Time varying heat loads are applied on power amplifiers on Downlink and Uplink for testing purpose. GPS is on during entire testing. Heat dissipation in magnetorquers has been neglected as for testing, very small amount of current will be used.

## 5.2 Heat Loads

### 5.2.1 Constant Heat Loads

| PCB | Heat dissipated(W) |
|---|---|
| OBC | 0.1425 |
| Beacon | 0.0425 |
| Beacon Power Amplifier | 1.7 |
| Downlink | 0.0836 |
| Sun Board | 0.025295 |
| Uplink | 0.14917 |
| LNA | 0.055 |
| GPS | 2 |
| Battery Box | 0.08 |

Table 5.1: Heat Loads: Thermovac

### 5.2.2 Variable Heat Loads for 3 hrs Soak

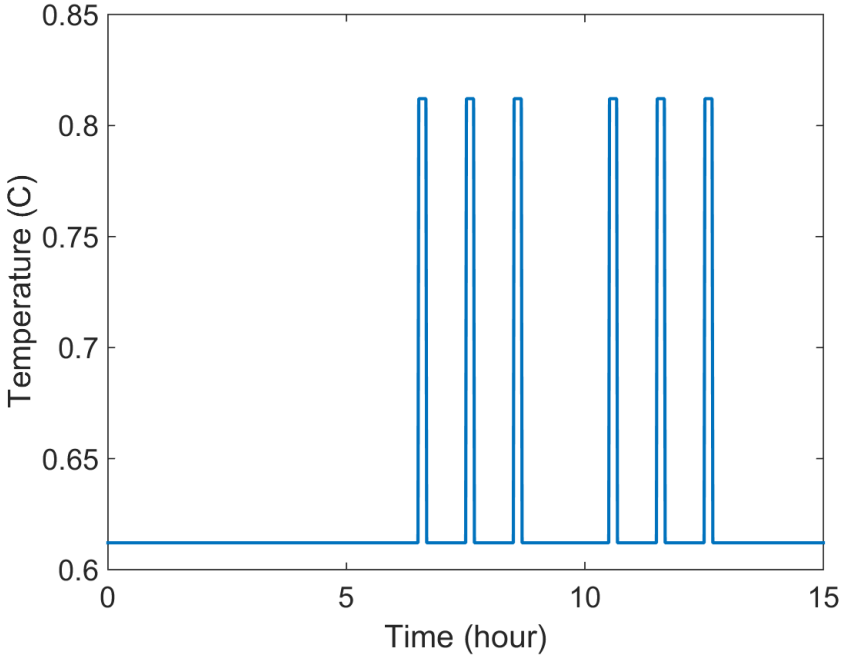


Figure 5.3: Heat Load on Power Board: Thermovac Testing

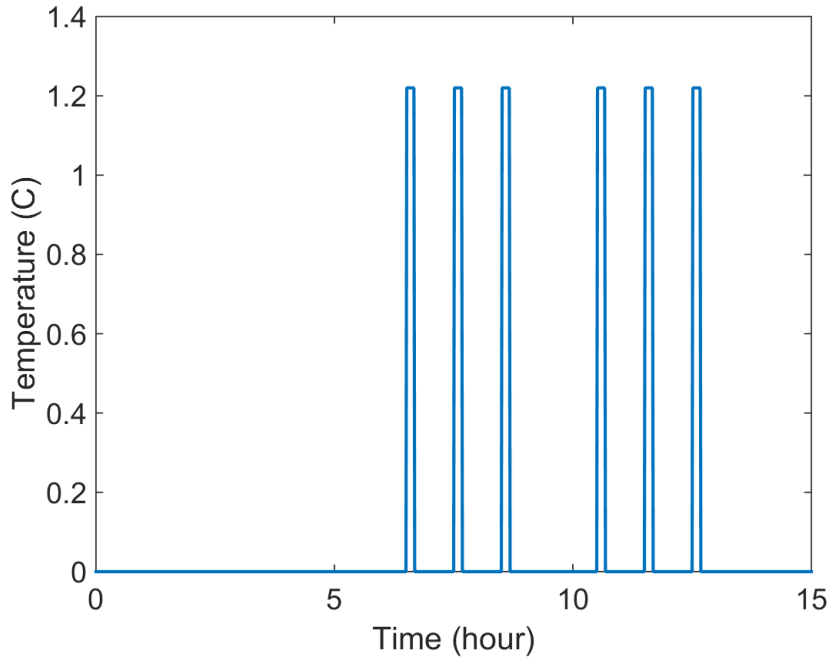


Figure 5.4: Heat Load in Power Amplifier on Downlink: Thermovac Testing

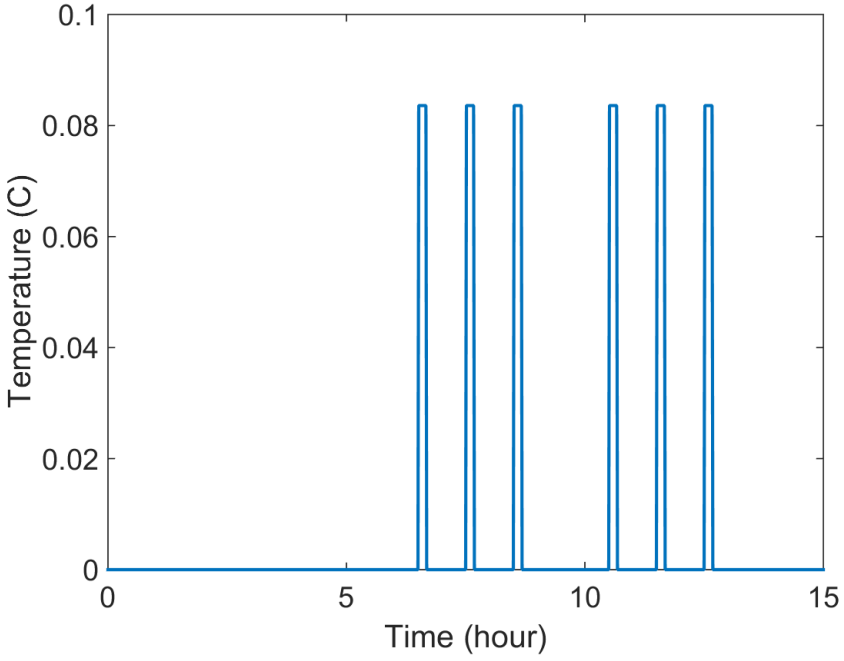


Figure 5.5: Heat Load in Downlink Board: Thermovac Testing

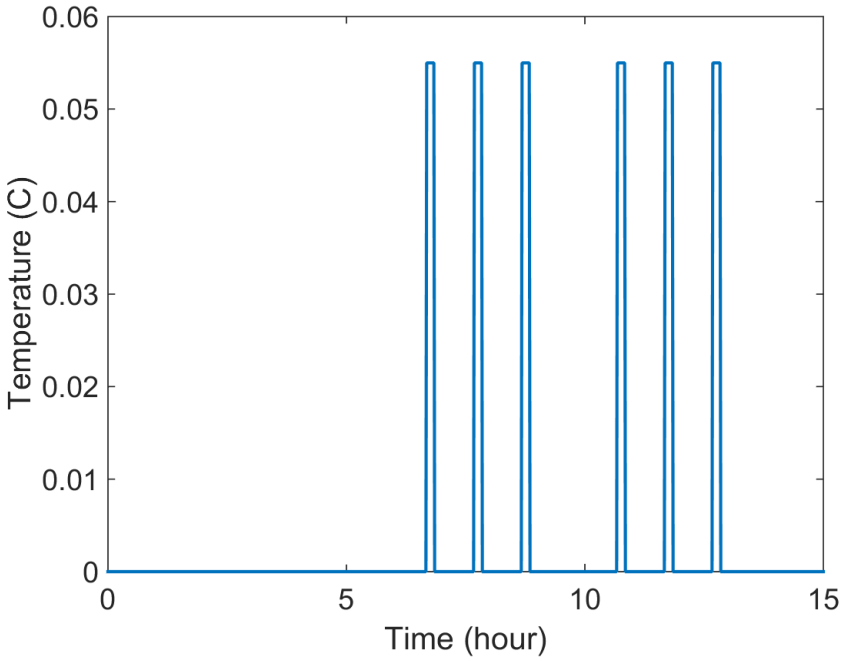


Figure 5.6: Heat Load in LNA on Uplink: Thermovac Testing

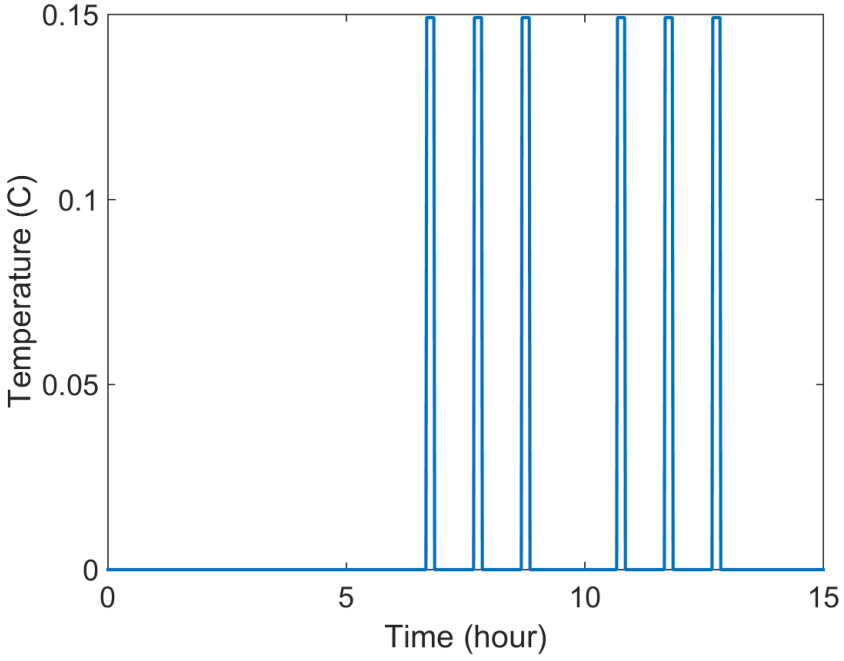


Figure 5.7: Heat Load in Uplink Board: Thermovac Testing

## 5.3 Results

| | 3 hrs Soak | | 4 hrs Soak | |
|---|---|---|---|---|
| **Components** | **Min** | **Max** | **Min** | **Max** |
| Zenith Solar Panel | -4 | 50.5 | -5.2 | 51.3 |
| Sunside Solar Panel | -4.3 | 50.3 | -5.6 | 51.1 |
| Leading Solar Panel | -4.5 | 50.3 | -5.8 | 51.4 |
| Lagging Solar Panel | -4.1 | 50.7 | -5.3 | 51.6 |
| Zenith Side Panel | 0 | 51.2 | -1.6 | 52.5 |
| Sunside Side Panel | -0.3 | 50.9 | -2.2 | 52.2 |
| Leading Side Panel | -0.6 | 50.8 | -2.4 | 52 |
| Lagging Side Panel | 0.1 | 51.5 | -1.6 | 52.8 |
| Nadir Side Panel | -0.9 | 50.8 | -2.8 | 51.9 |
| Anti-Sunside Side Panel | 0.2 | 51.8 | -1.7 | 52.9 |
| Power Board | 5.1 | 54.2 | 3.5 | 55.5 |
| OBC Board | 1.4 | 51.9 | -0.4 | 53.2 |
| ADC Board | 1 | 51.6 | -0.9 | 52.9 |
| Uplink Board | 0.2 | 51.1 | -1.8 | 52.7 |
| Downlink Board | -0.1 | 51.1 | -1.9 | 52.3 |
| Beacon Board | 0.9 | 51.6 | -1.2 | 52.8 |
| LNA on Uplink Board | 0 | 51.3 | -1.8 | 52.5 |
| Power Amplifier on Downlink Board | -0.2 | 52.7 | -2 | 56.1 |
| Power Amplifier on Beacon Board | 6.5 | 57.6 | 4.7 | 58.8 |
| Uplink Board below LNA | 0.1 | 51.3 | -1.7 | 52.6 |
| Beacon Board below Heat Sink | 5.9 | 56.9 | 4.1 | 58.1 |
| Downlink Board below Heat Sink | -0.2 | 52.1 | -1.9 | 55.5 |
| Battery Box | 0.5 | 51.2 | -1.4 | 52.5 |
| GPS | 2.5 | 53 | 0.5 | 54.4 |
| Magnetometer | 1.1 | 52.3 | -0.7 | 53.6 |
| Magnetorquer on Zenith | 0.6 | 51.4 | -1.5 | 52.2 |
| Magnetorquer on Sunside | -0.3 | 51 | -2.4 | 51.9 |
| Magnetorquer on Leading | -0.4 | 51 | -2.6 | 52 |
| Monopoles | 0.2 | 51.4 | -1.7 | 52.7 |

Table 5.2: Thermovac Result

**Inferences:**

- Temperature of battery box and other components towards the end of simulation at ambient temperature of $50^0$ C have crossed $50^0$ C. Since at steady state, heat generated inside satellite has to go to environment via radiation. So, as the satellite

tends towards steady state at hot soak, temperature of components has to increase beyond $50^0$ C.

- From result table, it can be seen that as we move from outside to inside, there exists a positive spatial temperature gradient inwards.
- Local maxima of temperature can be seen in plots of beacon and uplink boards which corresponds to the heat generation at that time in that particular component.

## 5.4 Temperature Plots for 3 hour Soak Profile:

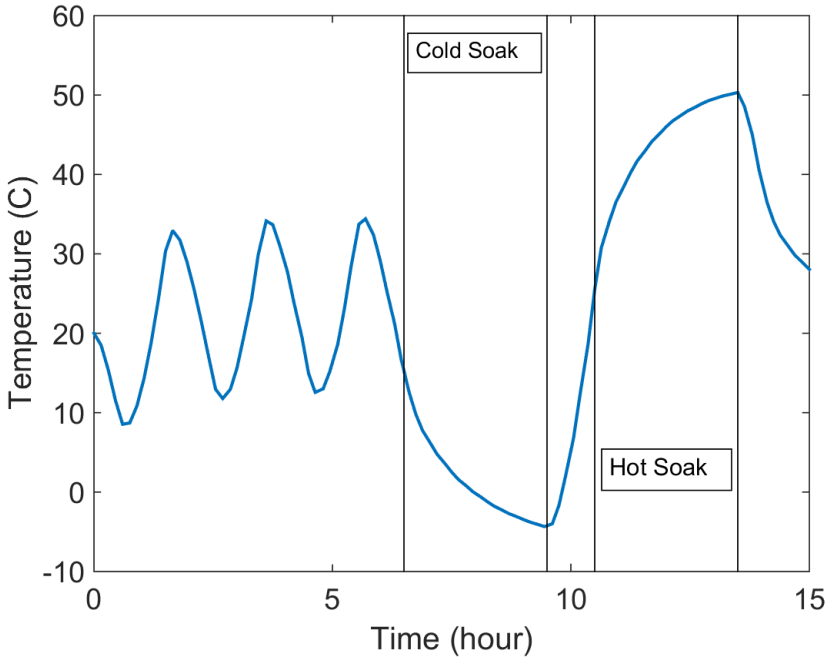


Figure 5.8: Temperature variation: Solar Panel

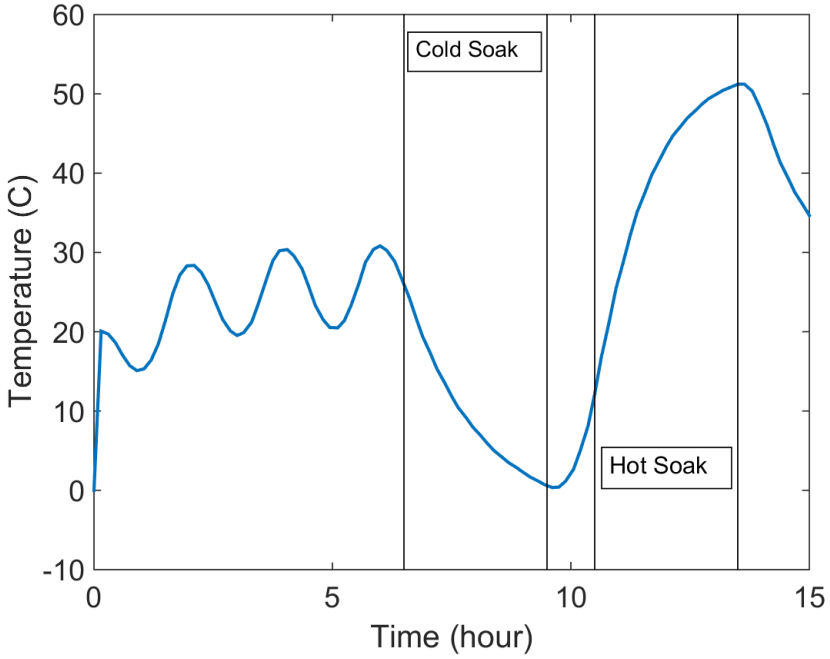


Figure 5.9: Temperature variation: Side Panel

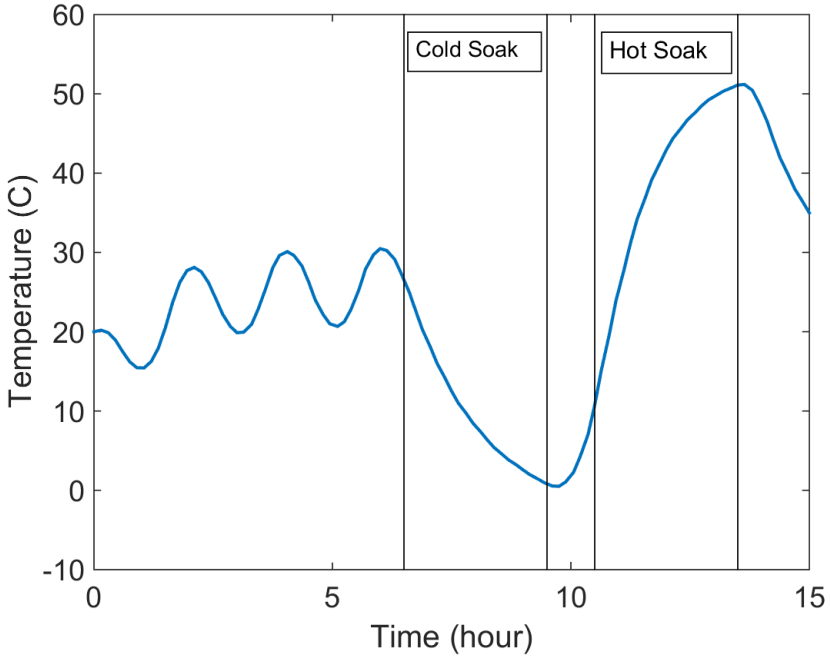


Figure 5.10: Temperature variation: Battery Box

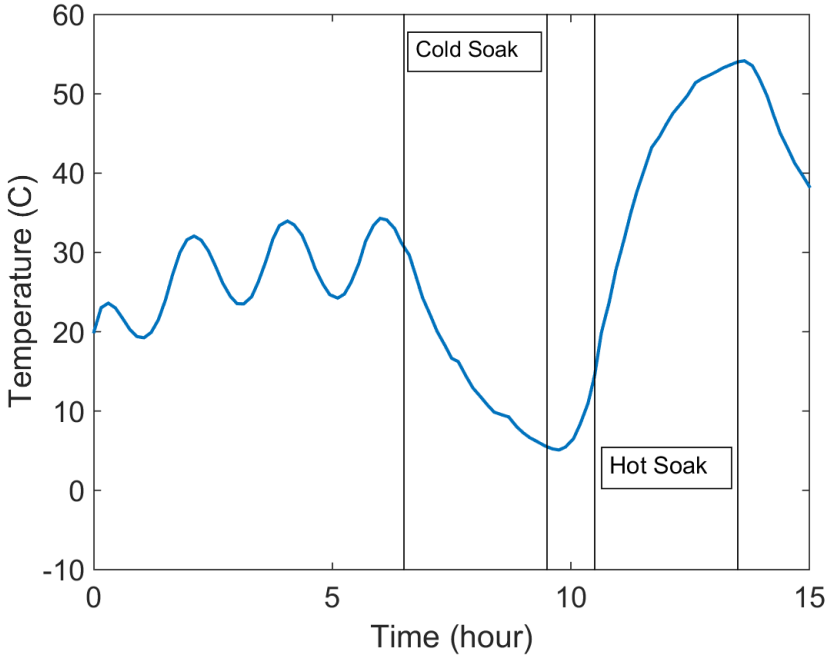


Figure 5.11: Temperature variation: Power Board

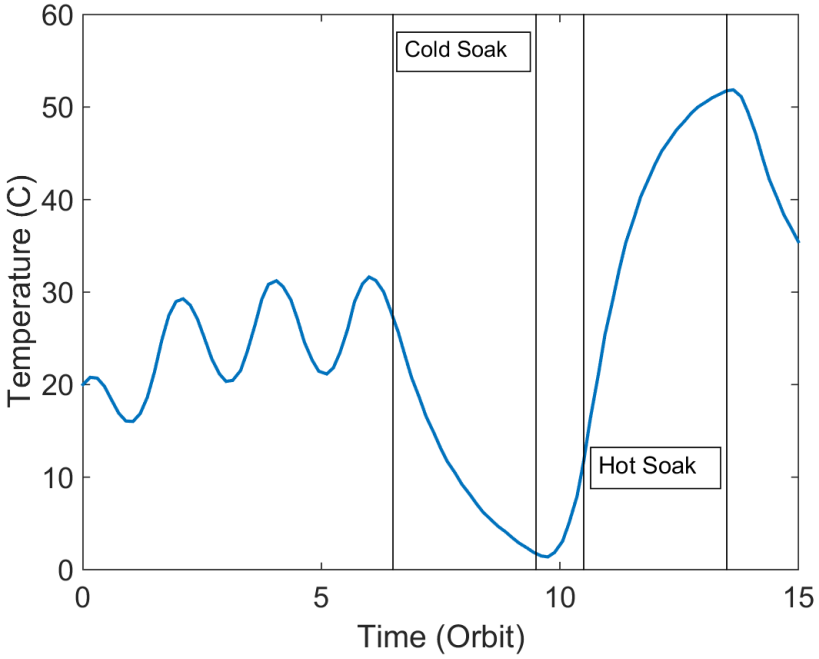


Figure 5.12: Temperature variation: OBC Board

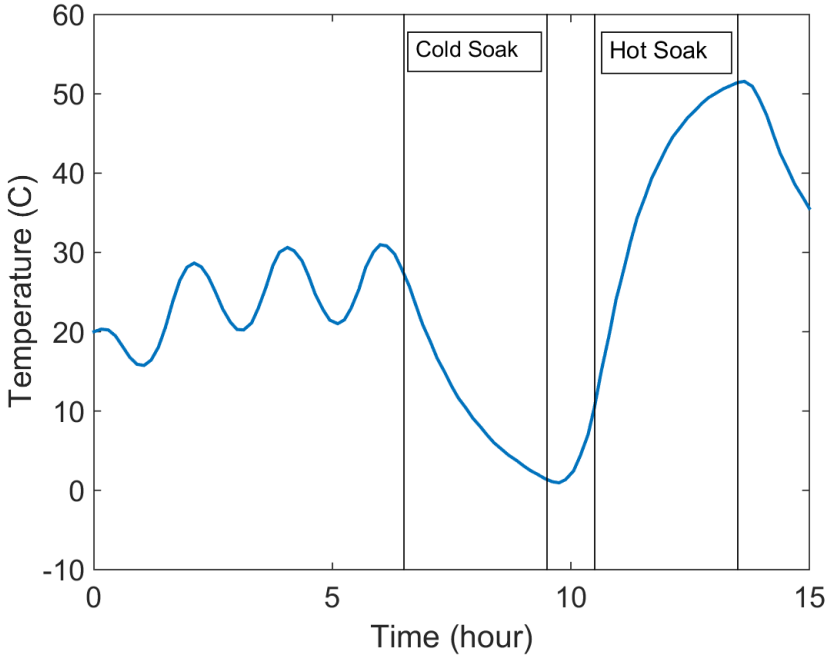


Figure 5.13: Temperature variation: Sunsensor Board

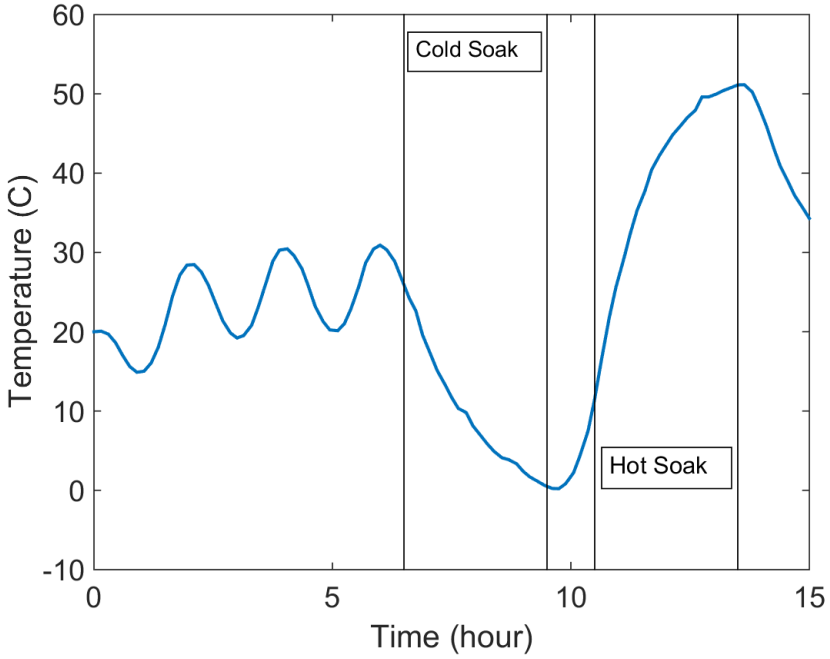


Figure 5.14: Temperature variation: Uplink Board

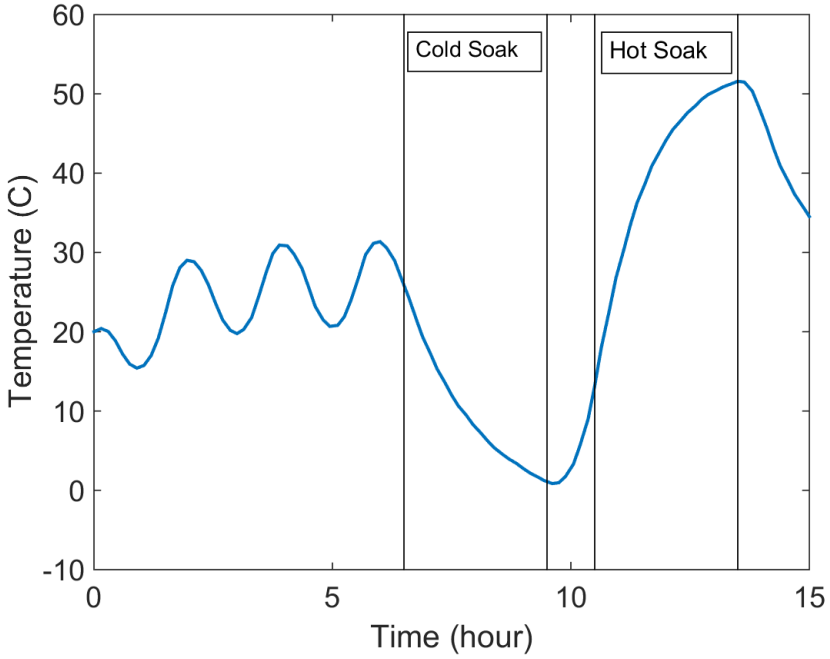


Figure 5.15: Temperature variation: Beacon Board

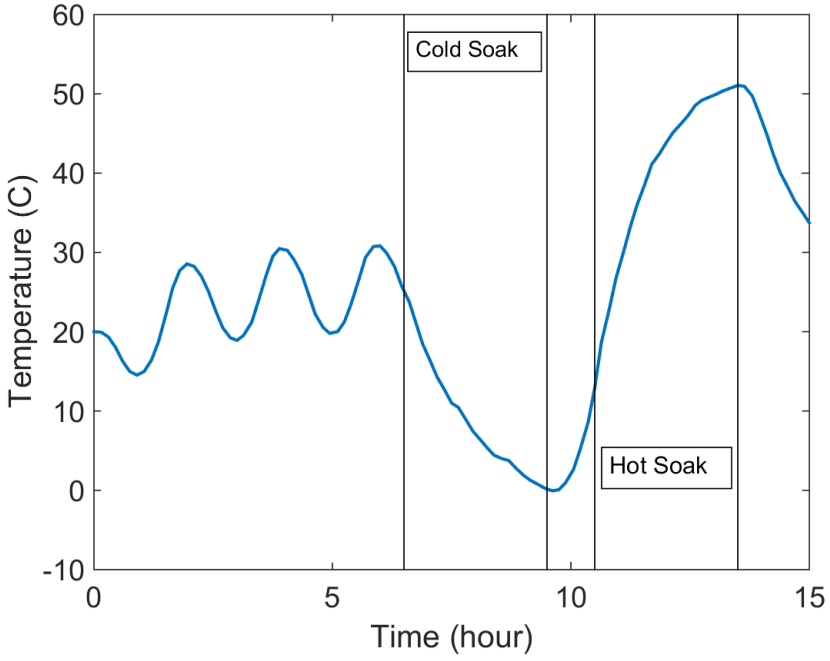


Figure 5.16: Temperature variation: Downlink Board

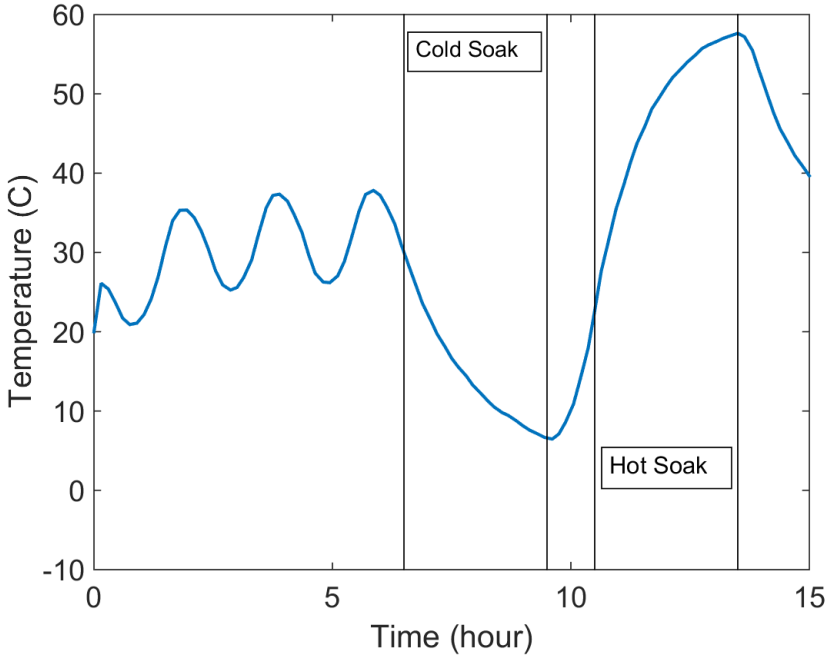


Figure 5.17: Temperature variation: Beacon Heat Sink

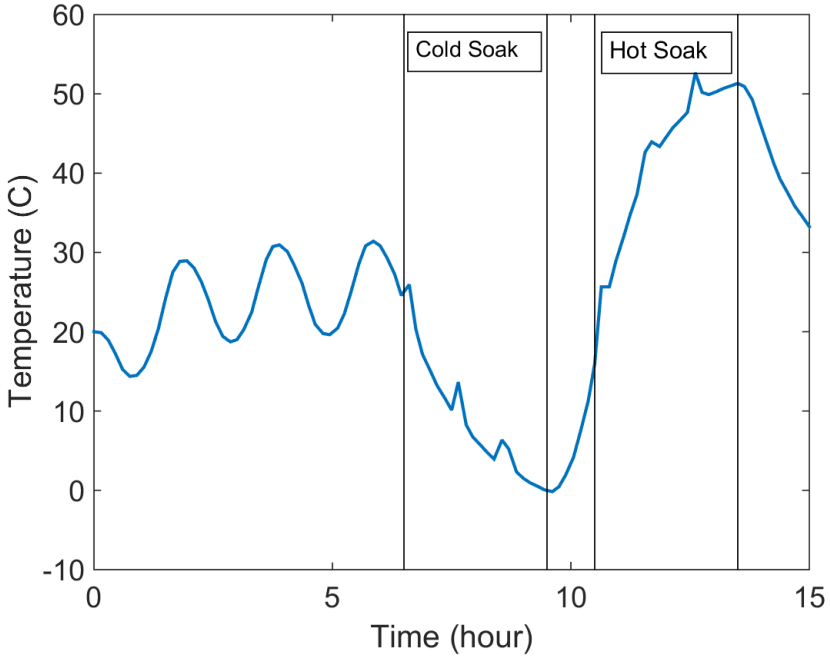


Figure 5.18: Temperature variation: Downlink Heat Sink

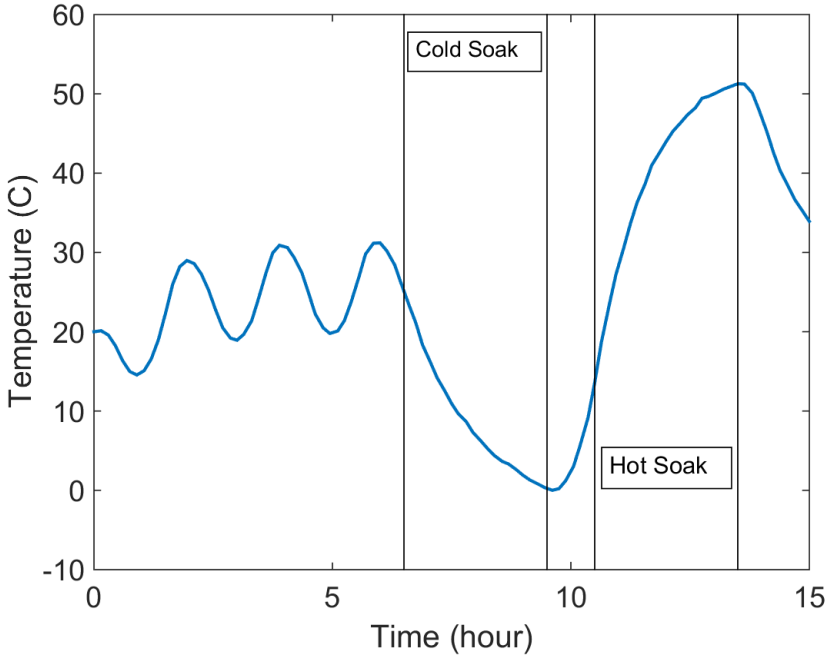


Figure 5.19: Temperature variation: Downlink Heat Sink

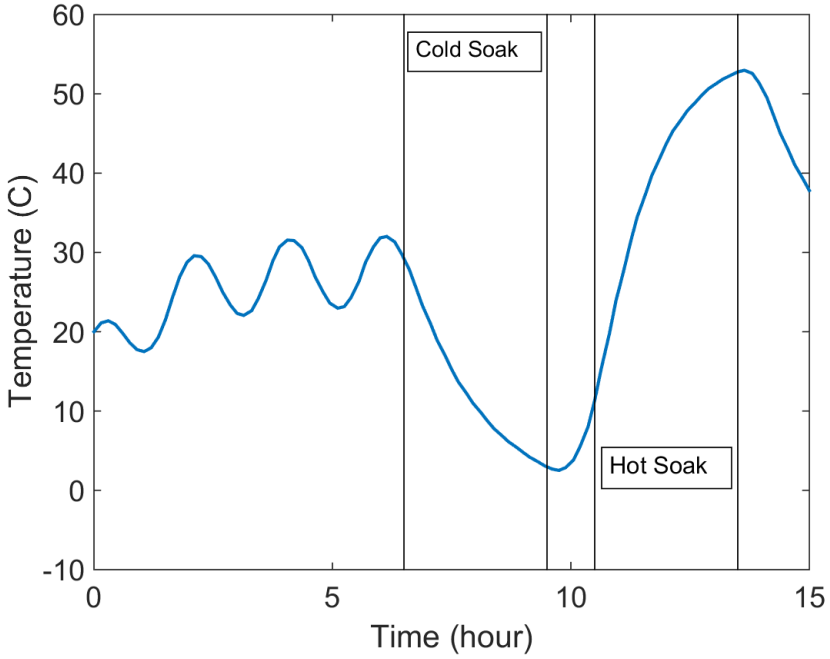


Figure 5.20: Temperature variation: GPS Box

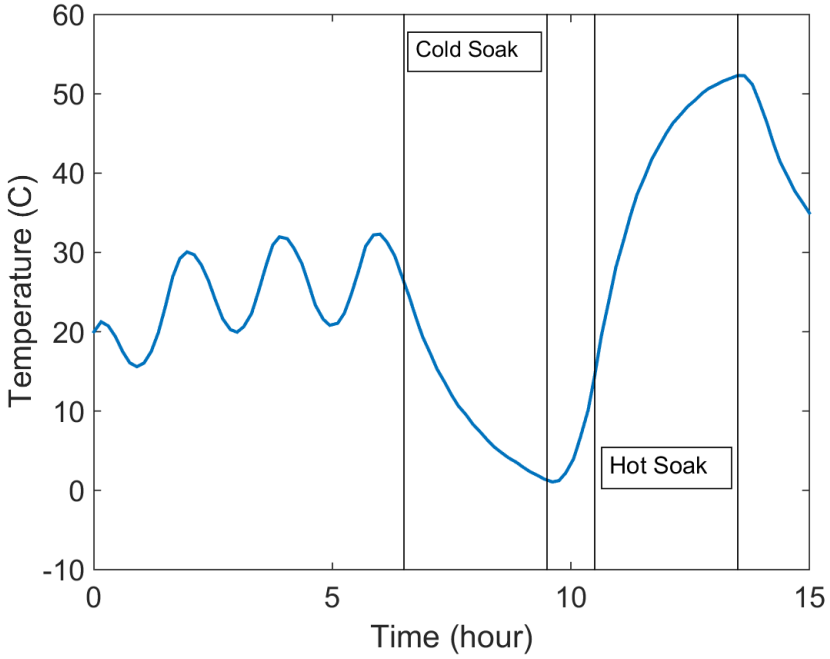


Figure 5.21: Temperature variation: Magnetometer

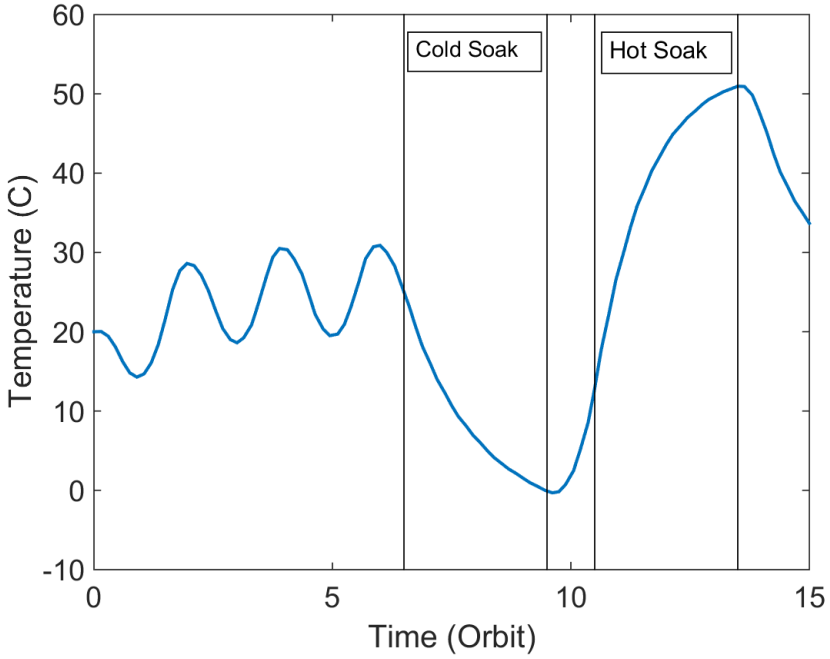


Figure 5.22: Temperature variation: Magnetorquer

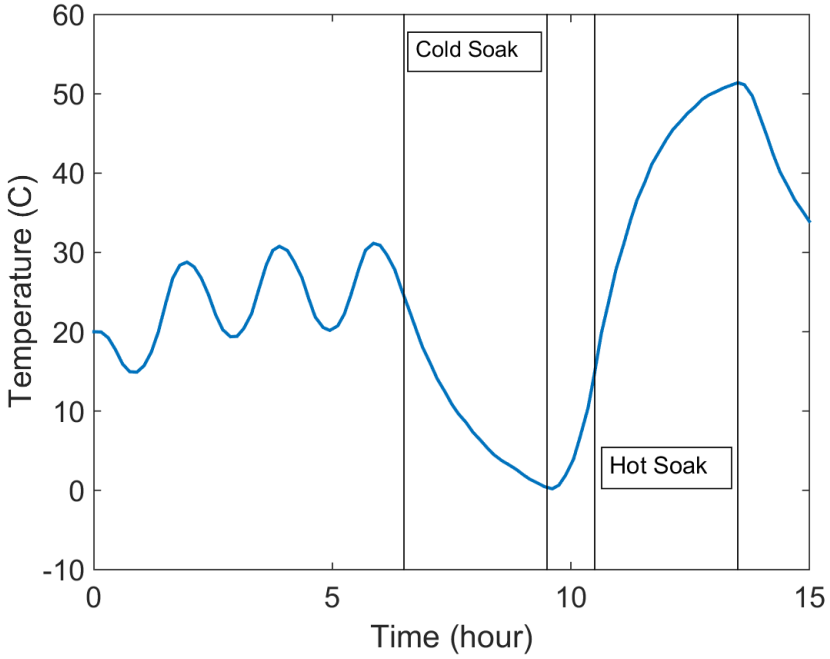


Figure 5.23: Temperature variation: Monopole

# Chapter 6

# Thermovac Testing

Temperature profile used for thermovac testing is given below

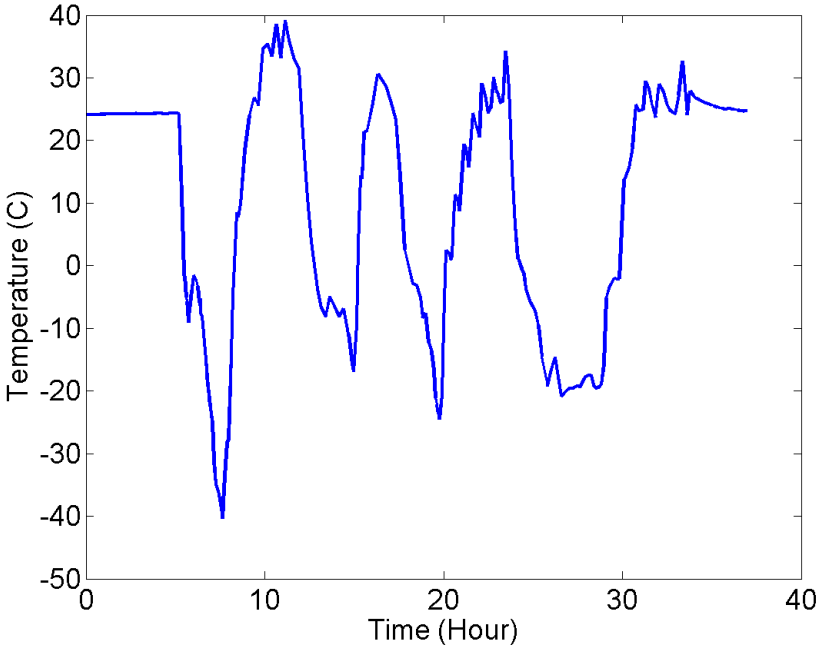


Figure 6.1: Temperature Profile for Thermovac testing

Above profile contains three transient cycles and after that a cold soak followed by a hot soak as planned. Initially upper and lower temperature limit was decided to be 50 $^0$ C and -10 $^0$ C respectively. During thermovac testing lower temperature limit was decided by battery and upper temperature limit was decided by power amplifier on beacon board. Ambient temperature was controlled in such a way that battery's temperature never decreases below 0 $^0$ C and Temperature of power amplifier on beacon board never rises beyond 40 $^0$ C.

| **Components** | **In- Orbit Temperatures** | | **Qualification value temperatures** | | **Observation values** | | **Margin** | |
|---|---|---|---|---|---|---|---|---|
| Temperature ($^0$C) | Min | Max | Min | Max | Min | Max | Min | Max |
| Battery | 14.8 | 22.2 | 4.8 | 32.2 | -7 | 33 | 11.8 | 0.8 |
| PA on Beacon | 13.4 | 21.7 | 3.4 | 31.7 | -15 | 60 | 18.4 | 28.3 |
| LNA on Uplink | 10.2 | 20 | 0.2 | 30 | -12 | 33 | 12.2 | 3 |
| PA on Downlink | 6.7 | 20 | -3.3 | 30 | -12 | 39 | 8.7 | 9 |

Table 6.1: Safety Margin

**Temperature plots of components during thermovac testing:** During thermovac testing of the satellite temperature of different components were monitored and stored. Following are the temperature plots of those components:

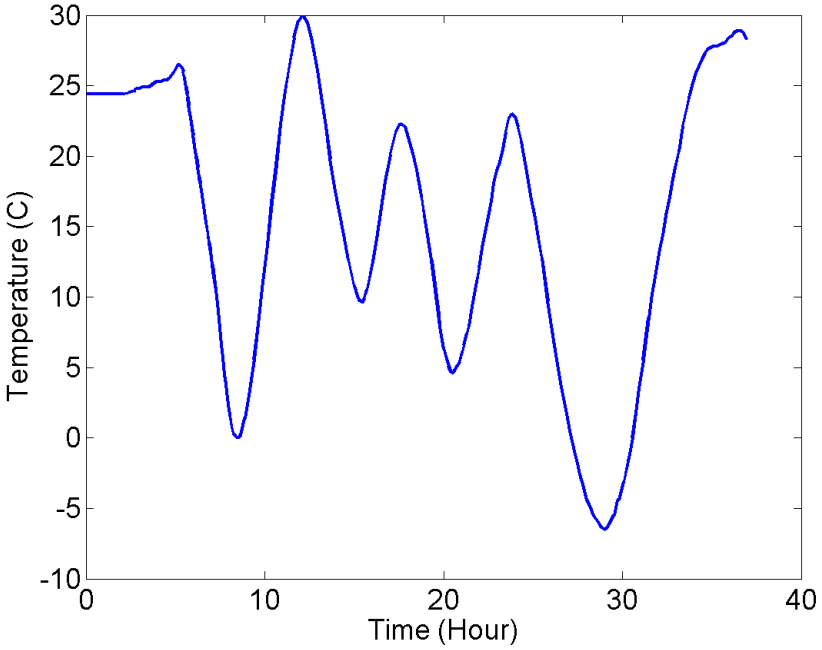


Figure 6.2: Temperature Variation: FE Ring

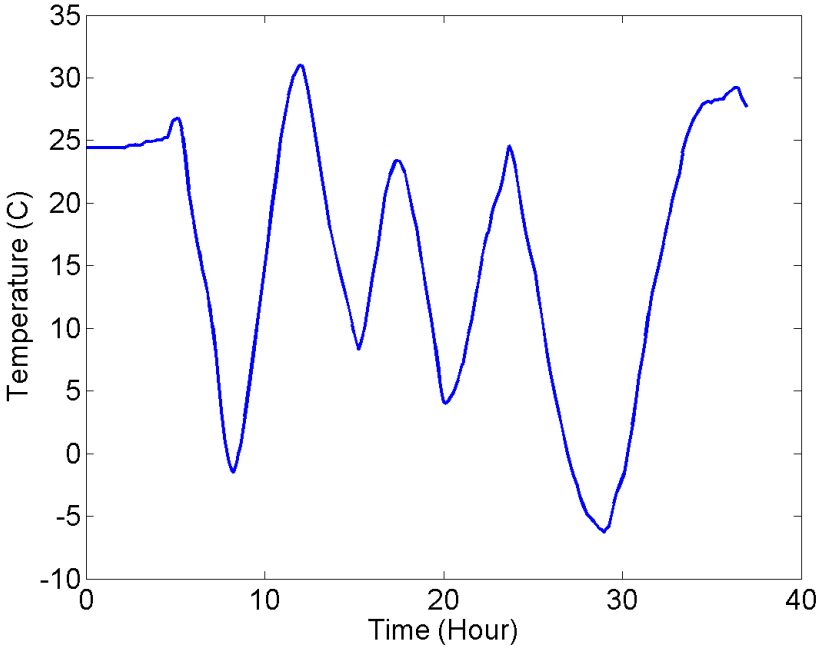


Figure 6.3: Temperature Variation: Anti-sunside

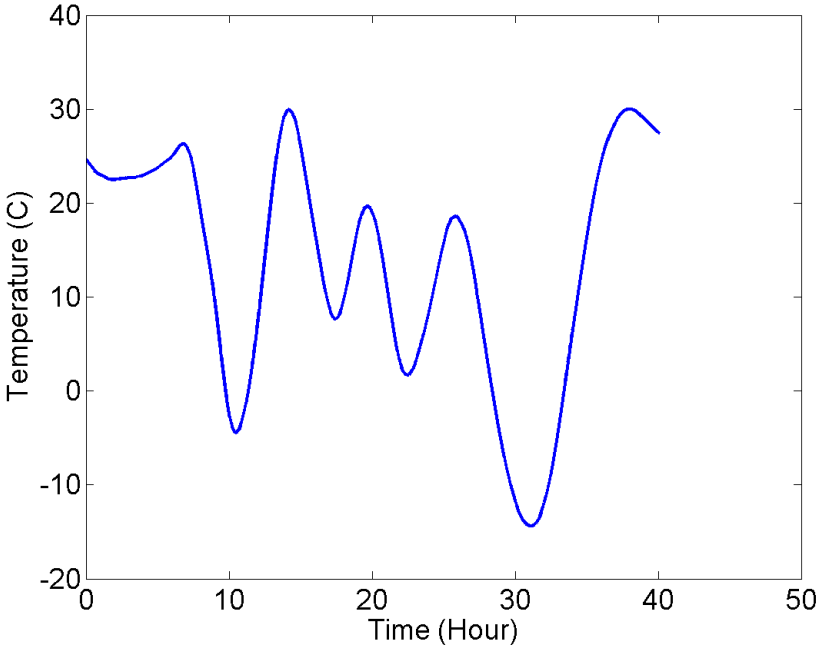


Figure 6.4: Temperature Variation: Battery

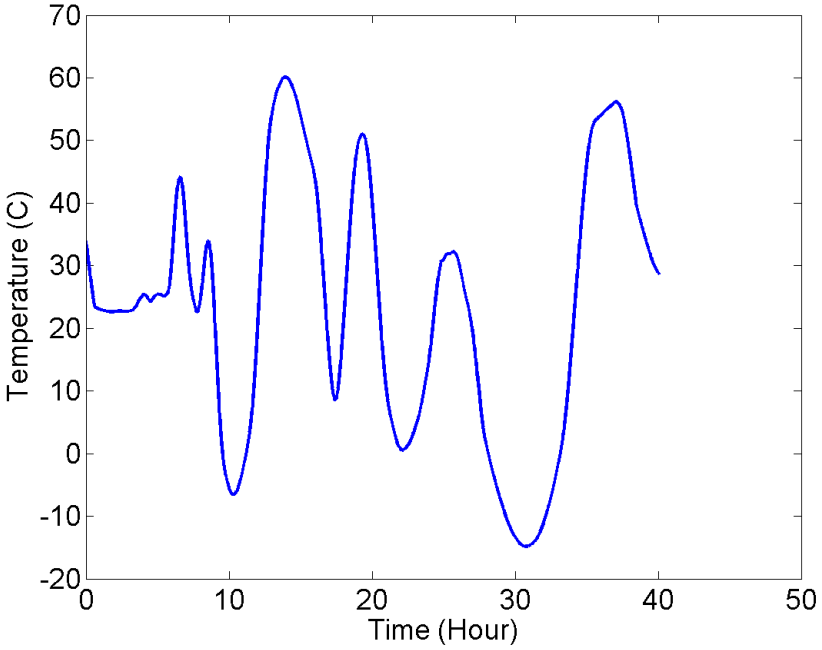


Figure 6.5: Temperature Variation: Power Amplifier on Beacon Board

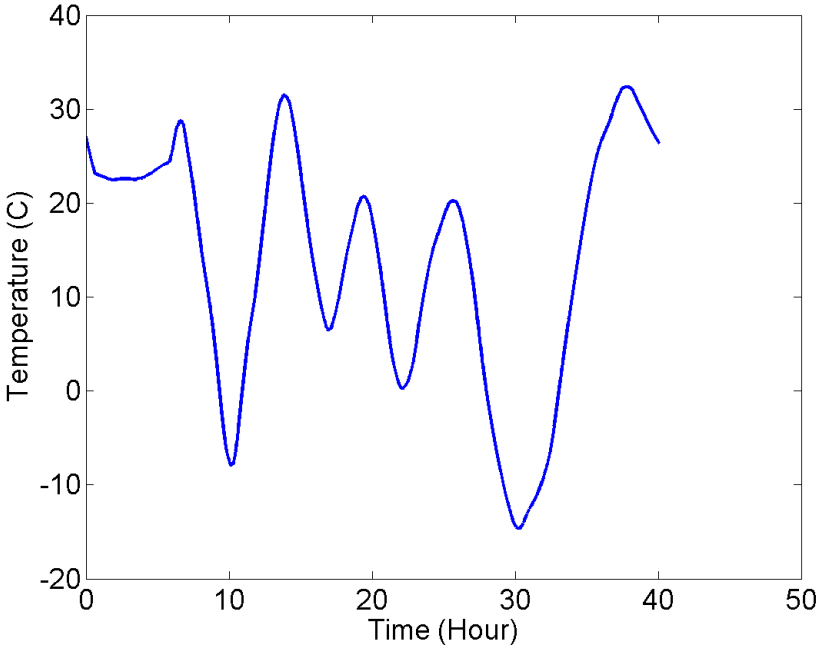


Figure 6.6: Temperature Variation: Power Amplifier on Downlink Board

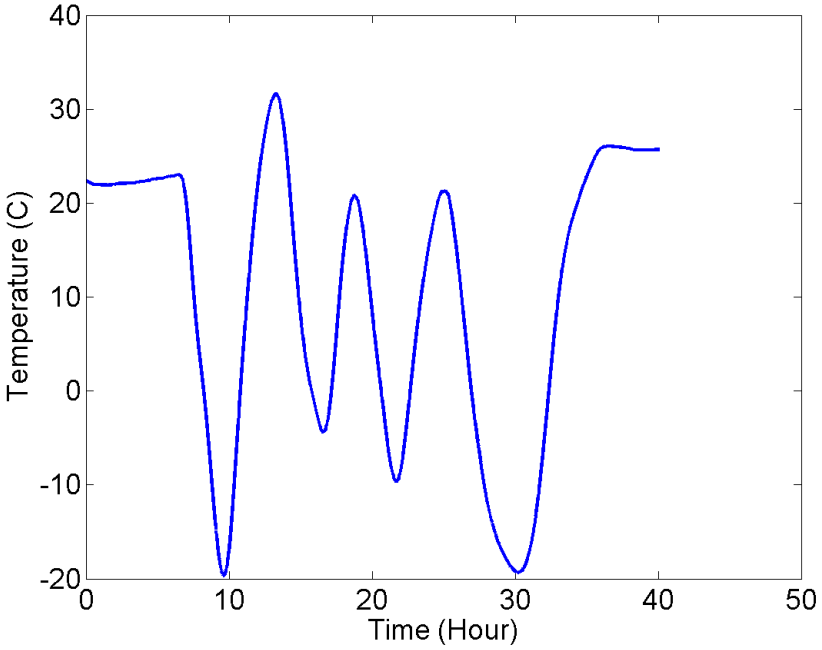


Figure 6.7: Temperature Variation: Lagging Solar Panel

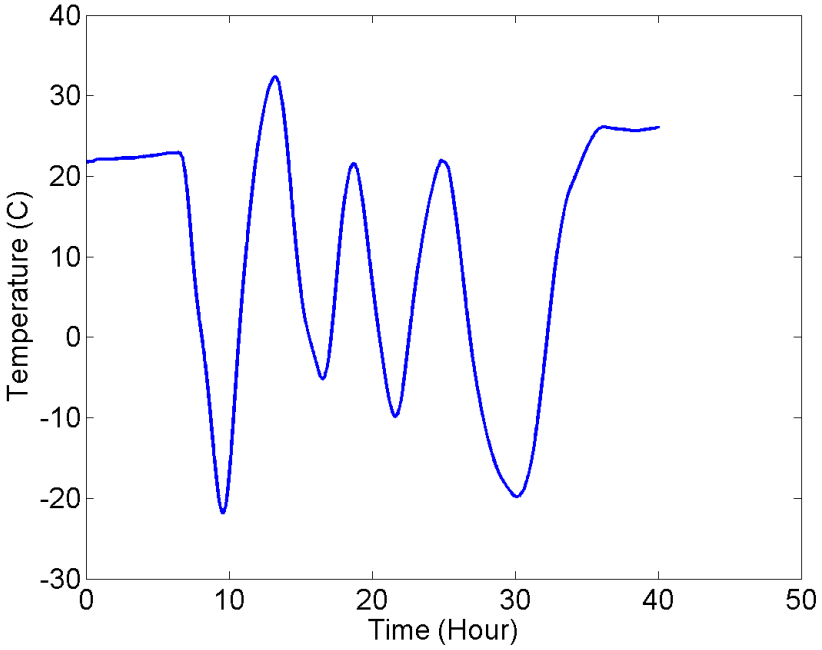


Figure 6.8: Temperature Variation: Leading Solar Panel

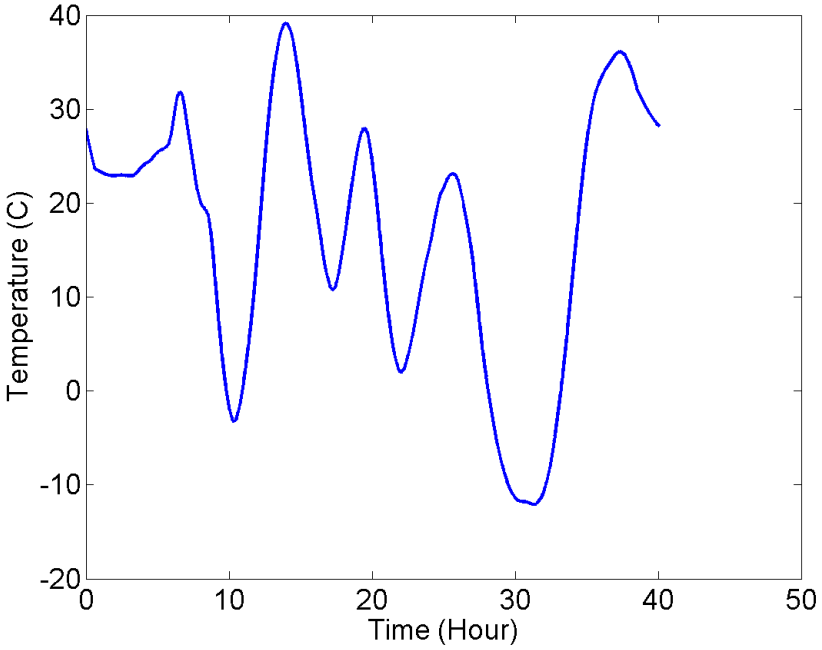


Figure 6.9: Temperature Variation: PTH for Power Amplifier on Beacon Board

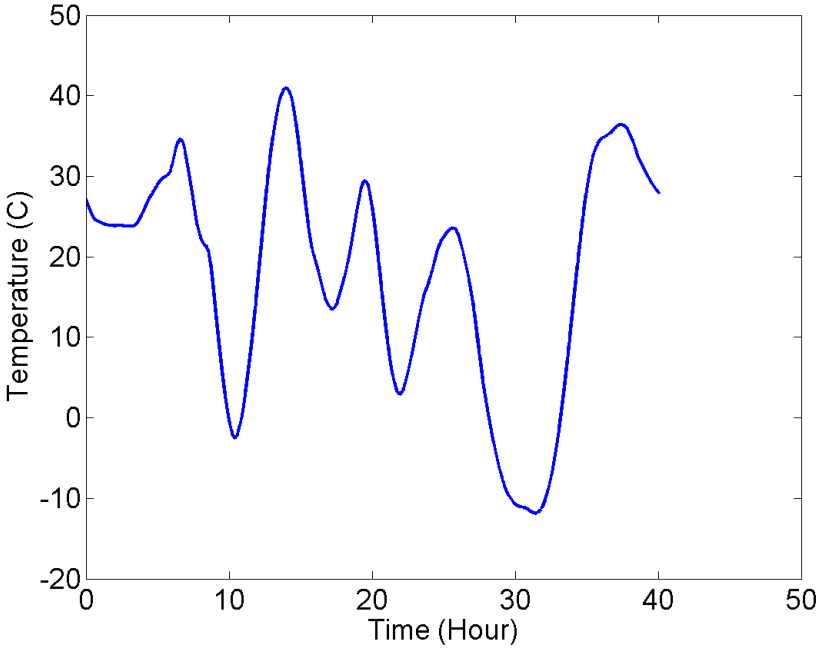


Figure 6.10: Temperature Variation: PTH for GPS Box

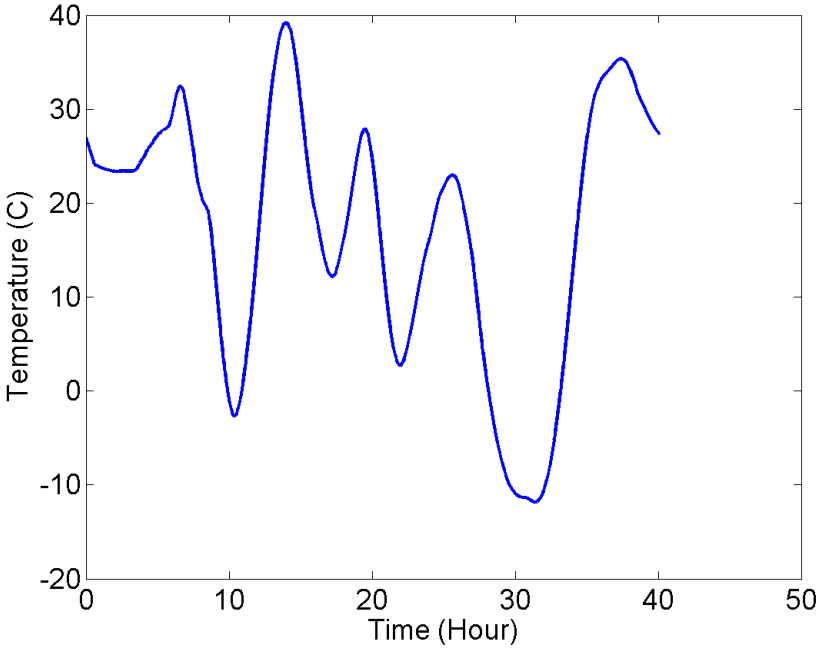


Figure 6.11: Temperature Variation: PTH for OBC Board

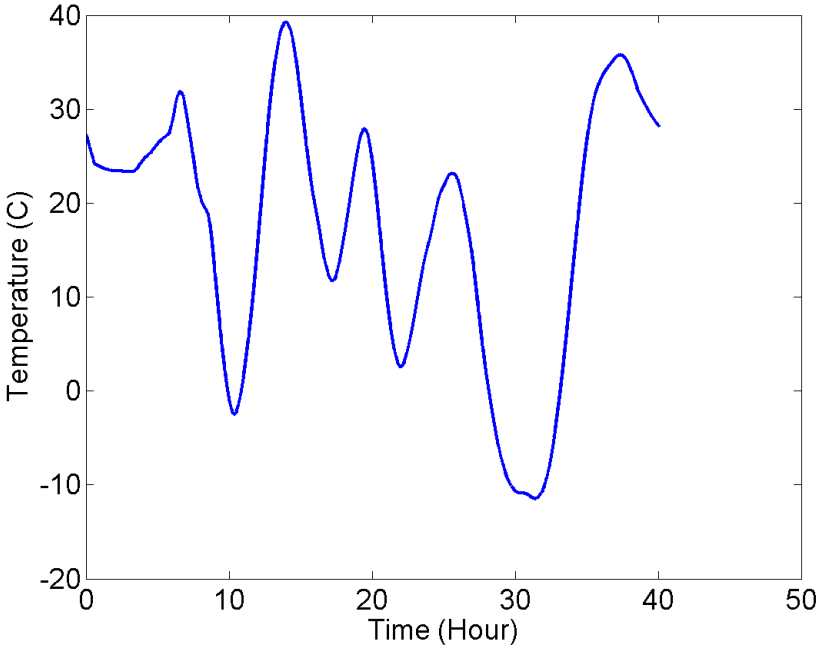


Figure 6.12: Temperature Variation: PTH for magnetometer

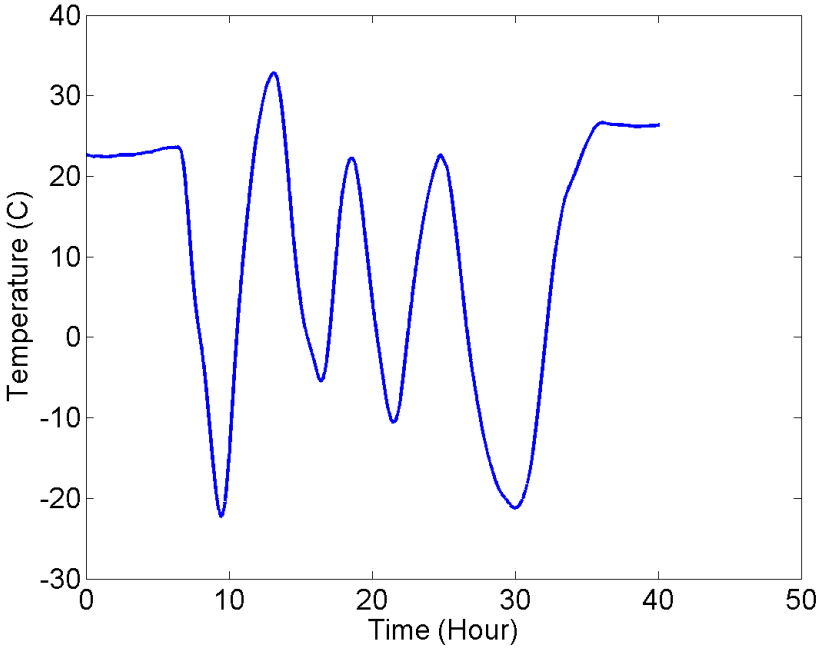


Figure 6.13: Temperature Variation: Sun-side Solar Panel

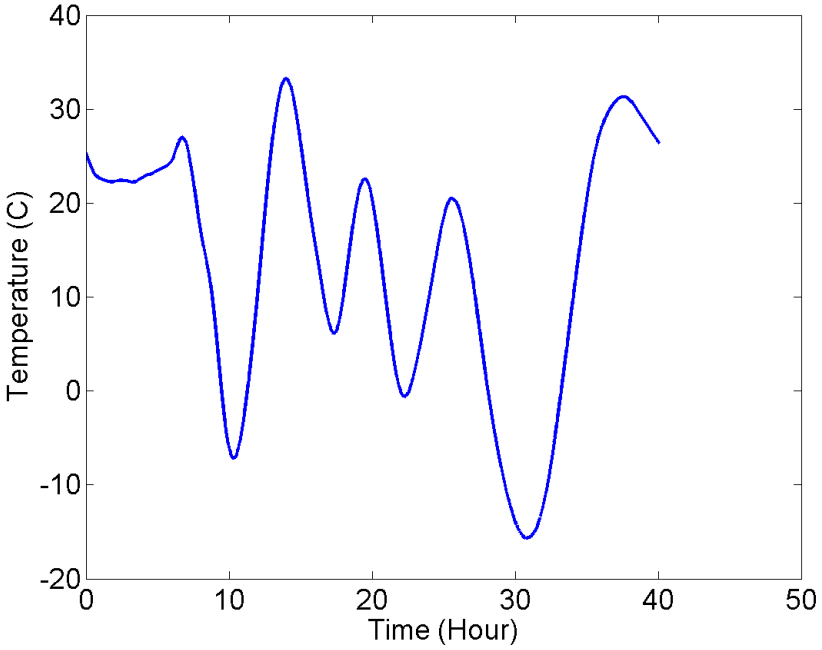


Figure 6.14: Temperature Variation: LNA on Uplink Board

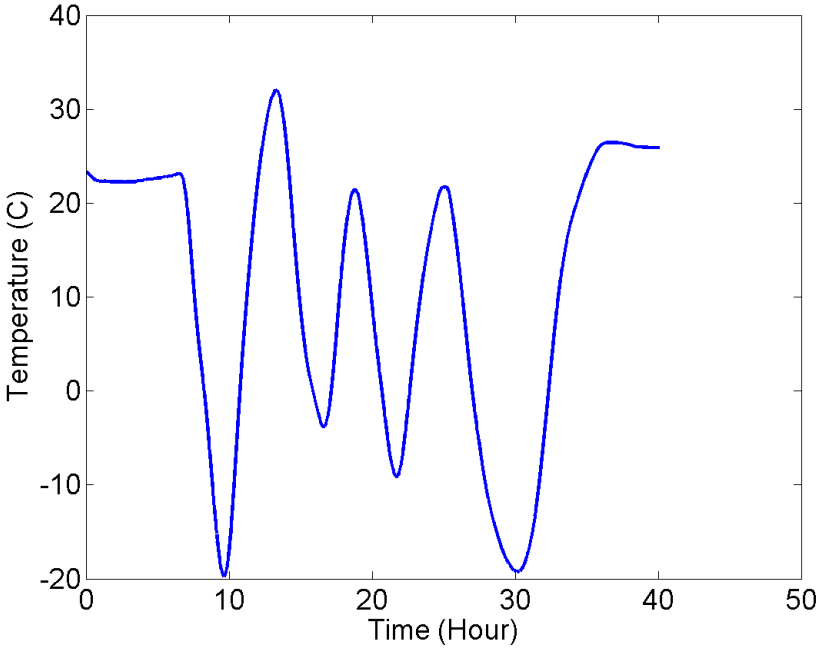


Figure 6.15: Temperature Variation: Zenith Solar Panel

1. Max and Min temperature observed for the components during thermovac were inside their operating range.

2. Qualification level temperatures were set having +10/-$10^0$ C to the in-orbit temperature observed.

3. All the components were tested for qualification level temperature with positive safety margin.

## 6.1 Comparison of Thermovac Simulation with Testing

| Component | Tvac Testing | | Tvac Simulation | |
|---|---|---|---|---|
| | Min | Max | Min | Max |
| Battery | -14.4 | 30 | 0.5 | 51.2 |
| Power Amplifier on Beacon | -14.8 | 60.1 | 6.5 | 57.6 |
| Power Amplifier on Downlink | -14.6 | 32.4 | -0.2 | 52.7 |
| LNA on Uplink | -15.7 | 33.2 | 0 | 51.3 |
| Lagging Side Panel | -19.6 | 31.6 | 0.1 | 51.5 |
| Leading Side Panel | -21.8 | 32.2 | -0.6 | 50.8 |
| Sunside Side Panel | -22.2 | 32.8 | -0.3 | 50.9 |
| Zenith Side Panel | -19.7 | 32 | 0 | 51.2 |
| Fe Ring | -6.5 | 30 | -0.1 | 50.8 |
| Anti Sunside | -6.3 | 31 | 0.2 | 51.8 |

Table 6.2: Comparison of Temperature between Tvac Testing and Simulation

Thermovac simulation results does not match with thermovac testing due to following reasons:

- Thermovac profiles used are different
- Hot soak and cold soak lengths are different
- Thermovac simulation assumes that satellite assumes that is kept in space thus whatever heat is radiated by satellite does not come back. But in thermovac testing, heat radiated by satellite is reflected back to it by the walls of thermovac chamber.
- Kapton tape was applied on outer surface of the satellite at some places, thus reducing the heat transfer by radiation.

Due to above reasons another thermovac simulations were done after thermovac testing. In which, thermovac chamber along with base plate on which satellite is placed were modeled. Heat exchange between satellite, thermovac chamber and base plate has been taken into account. Thermovac profile for simulation is same as temperature profile used for testing.

**Model used for Thermovac Simulation:**

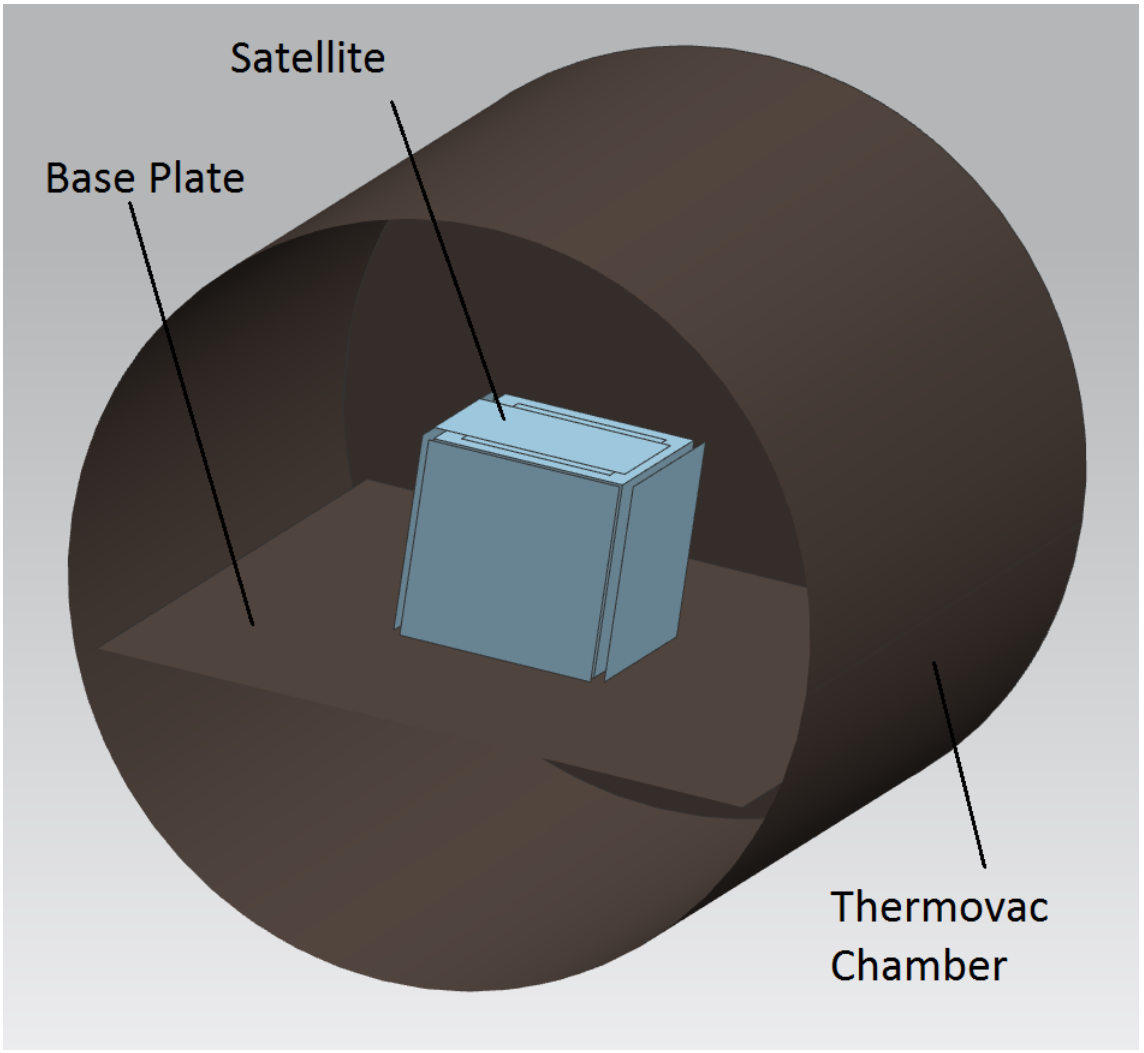


Figure 6.16: Section View: Satellite inside Thermovac Chamber

Dimension of Chamber: length = 1.2 m and Inner diameter = 1 m.
**Using new model, two new thermovac simulations were done:**

1. First simulation has been done for 7.38 hours. It starts from the time when testing was started and then calculated temperature for next 7.38 hours. Heat dissipation for electrical components has been applied according to actual testing. Temperature profile used for this simulation:

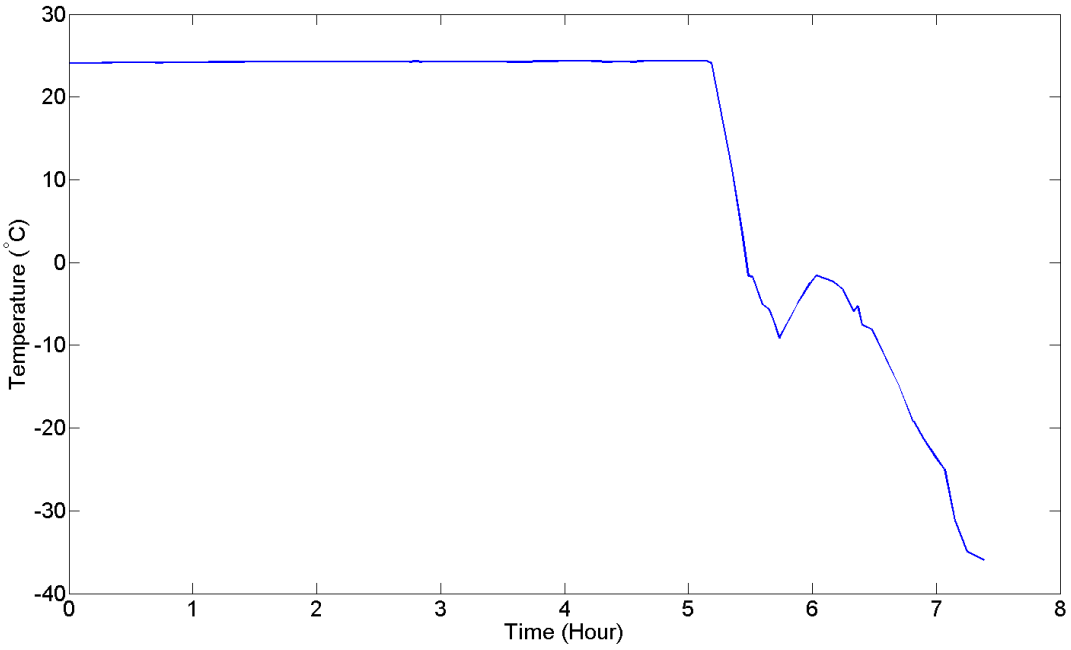


Figure 6.17: Temperature Profile used for simulation: first 7.38 hours of testing

**Comparison of Plots Obtained from Thermovac Simulation and Testing:**

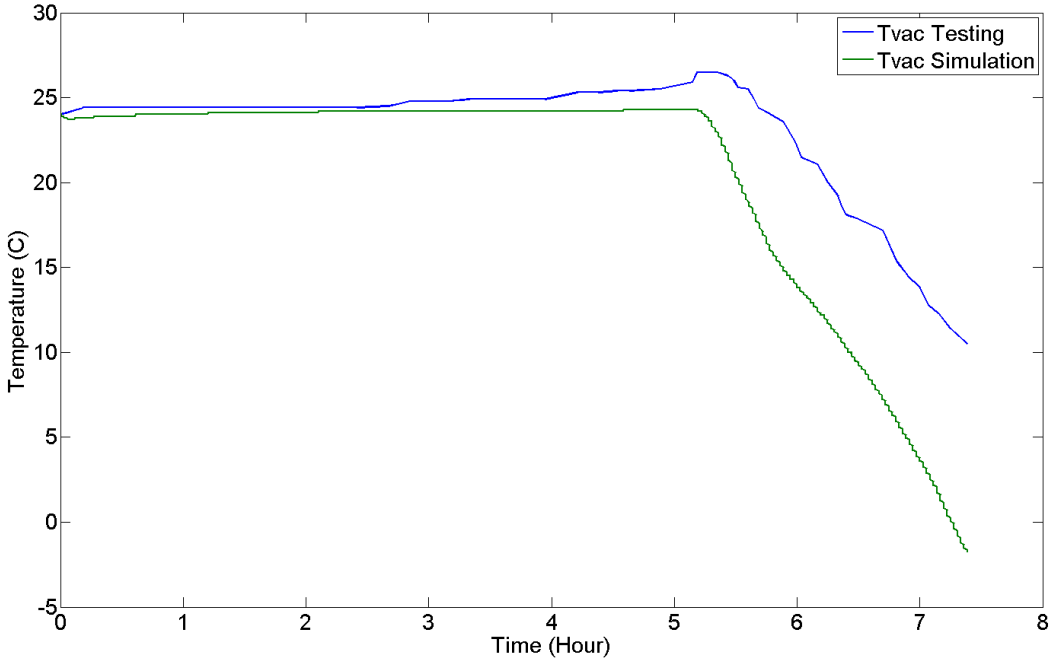


Figure 6.18: Temperature Plot: FE Ring

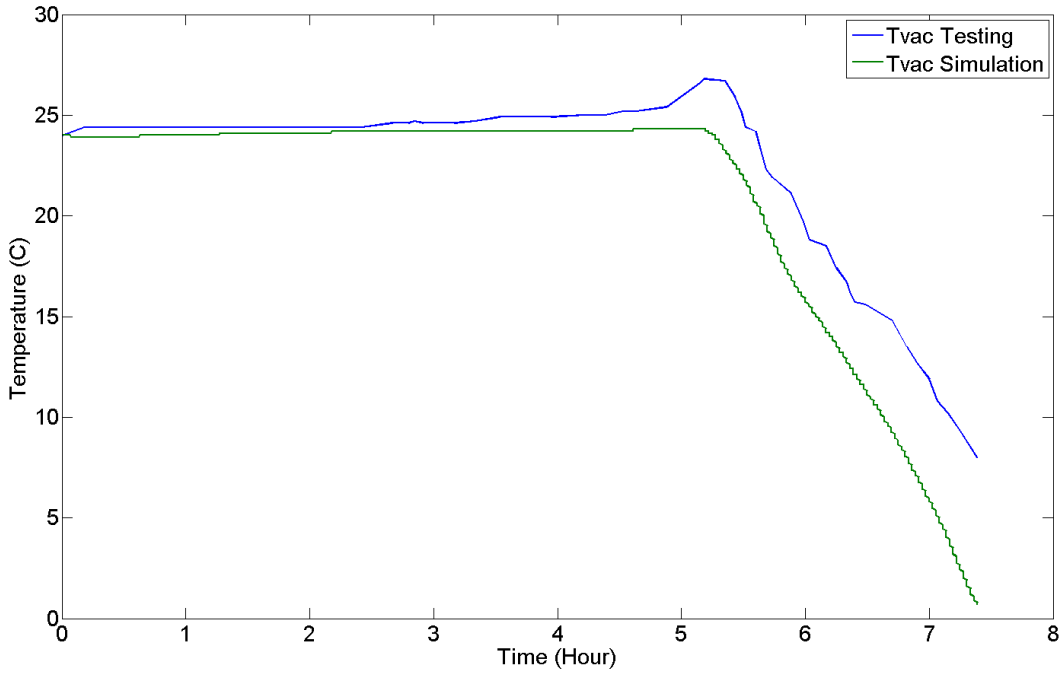


Figure 6.19: Temperature Plot: Anti-sunside

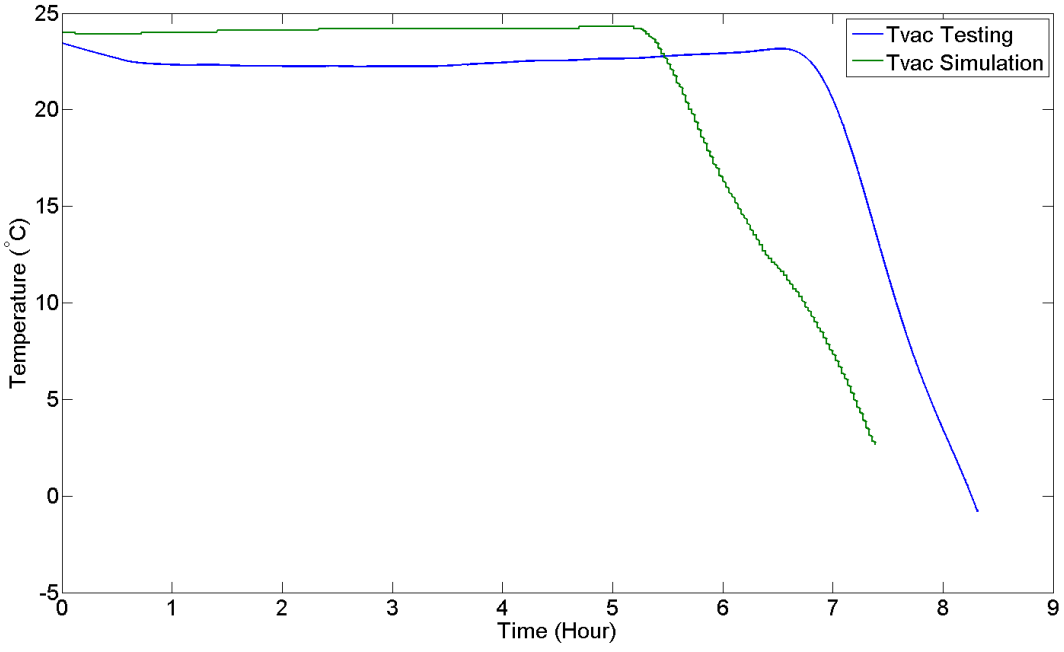


Figure 6.20: Temperature Plot: Zenith Solar Panel

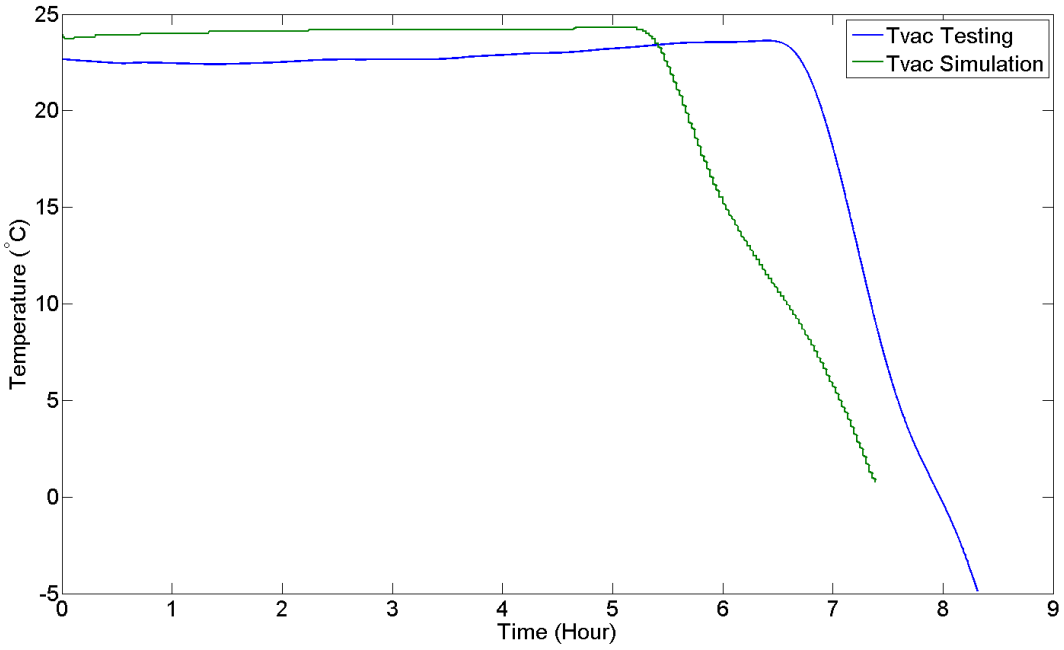


Figure 6.21: Temperature Plot: Sunside Solar Panel

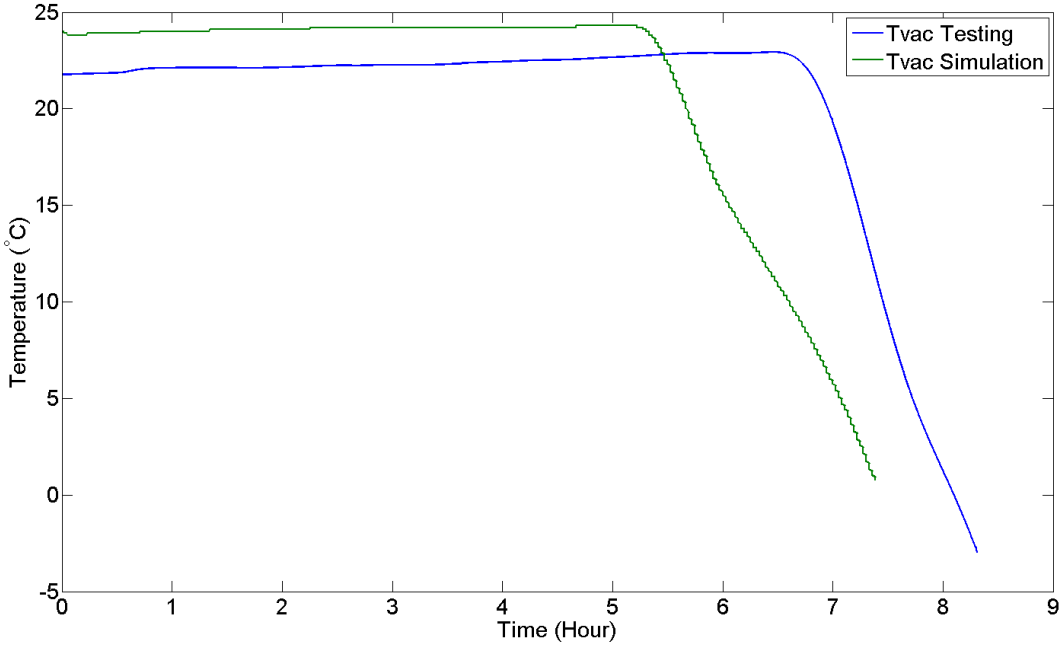


Figure 6.22: Temperature Plot: Leading Solar Panel

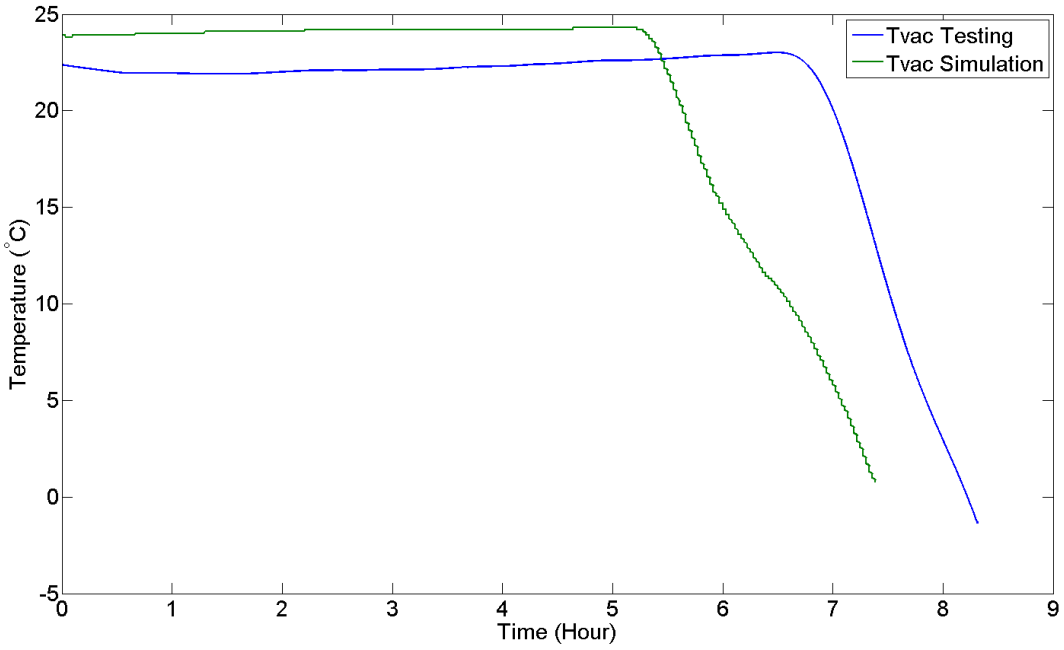


Figure 6.23: Temperature Plot: Lagging Solar Panel

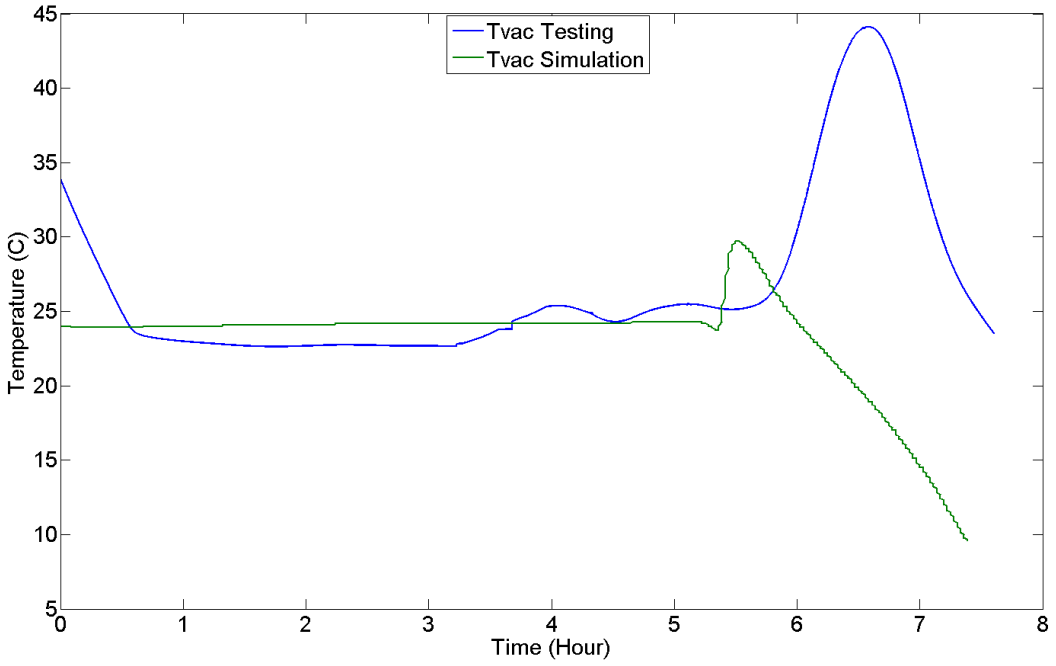


Figure 6.24: Temperature Plot: Power Amplifier on Beacon Board

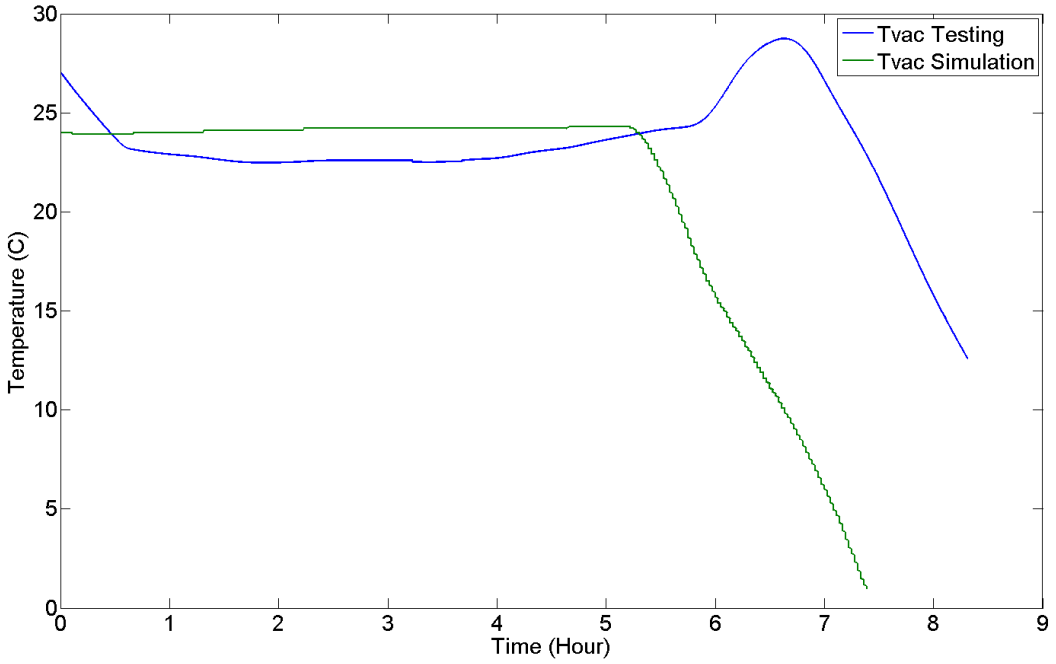


Figure 6.25: Temperature Plot: Power Amplifier on Downlink Board

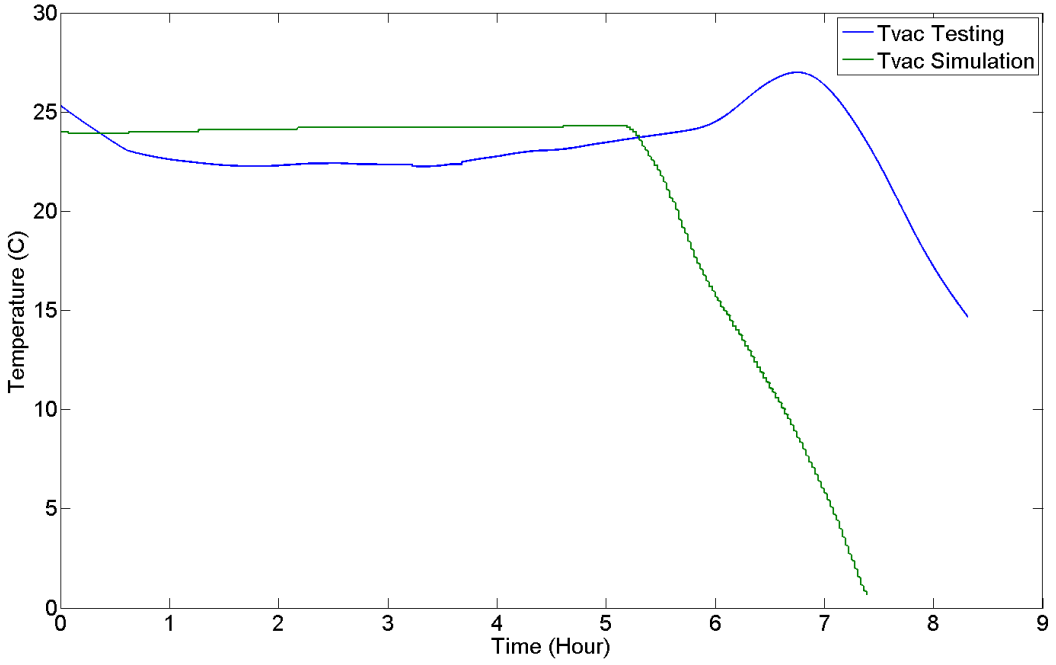


Figure 6.26: Temperature Plot: LNA on Uplink Board

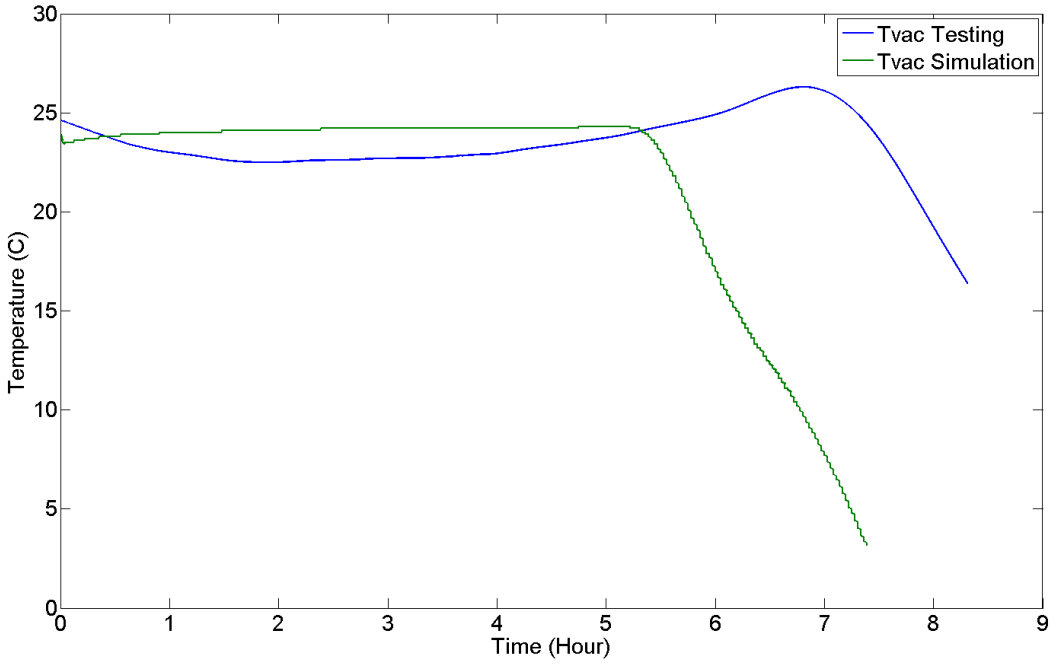


Figure 6.27: Temperature Plot: Battery

2. Hot Soak simulation: This simulation has been done for 2.6 hours, during which hot soak was performed. Heat dissipation for electrical components has been applied according to actual testing. Temperarature profile used for this simulation:

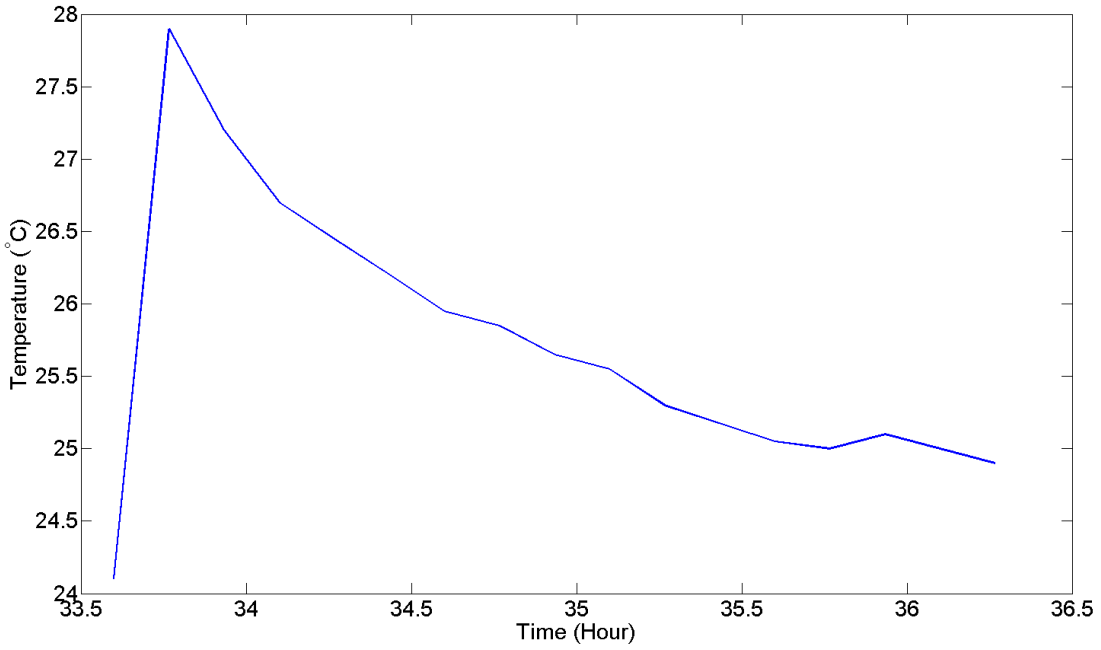


Figure 6.28: Temperature Profile used for simulation: During Hot Soak

**Comparison of Plots Obtained from Thermovac Simulation and Testing:**

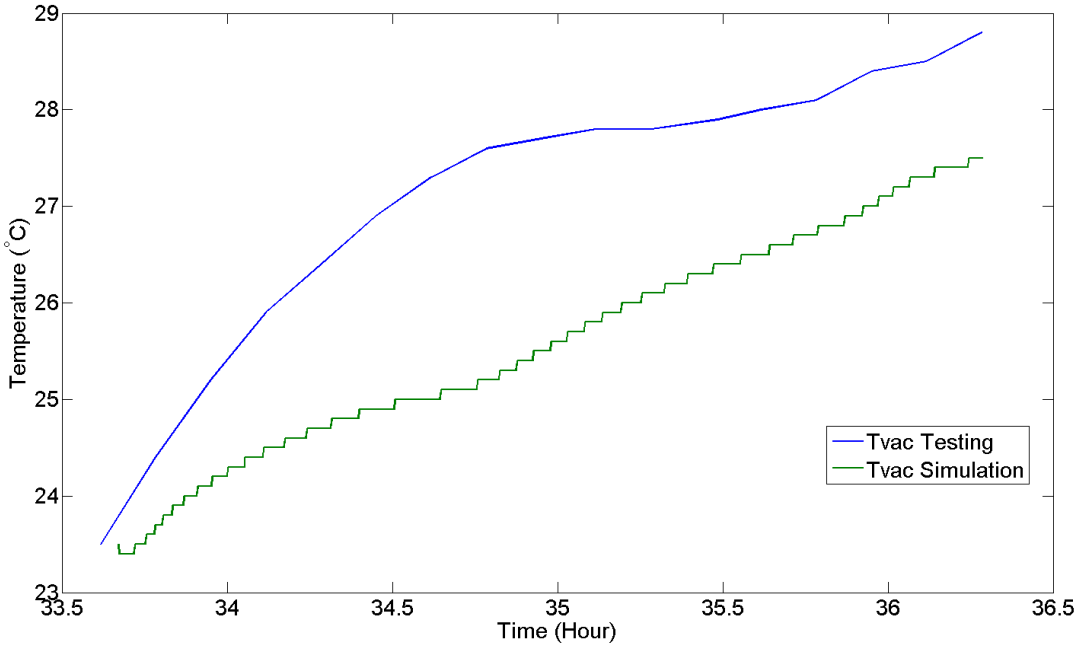


Figure 6.29: Temperature Plot: FE Ring

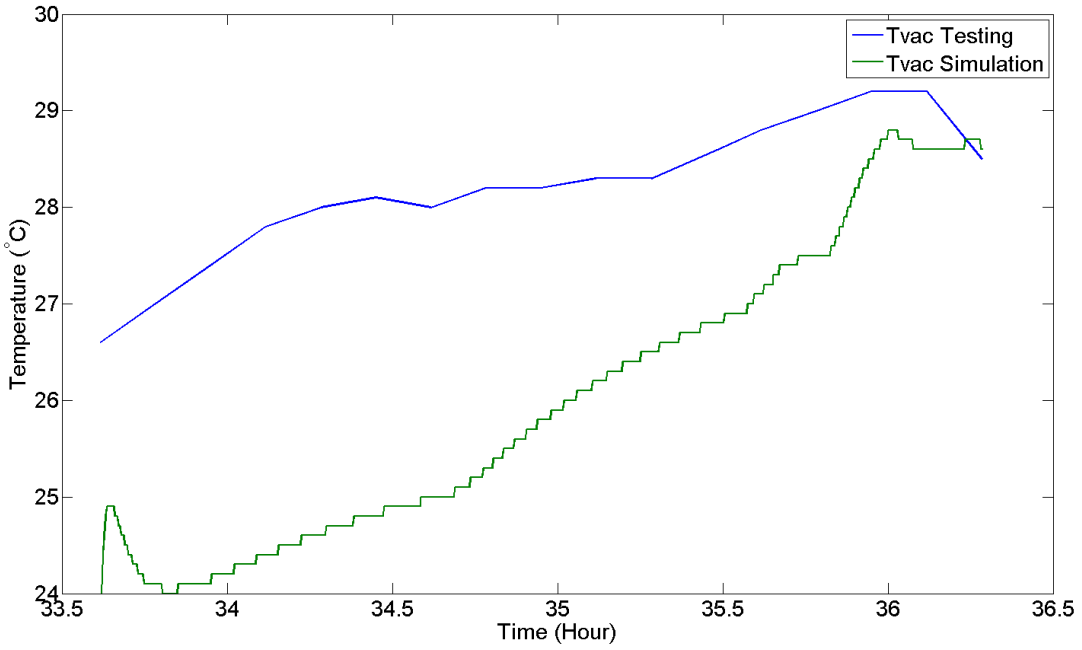


Figure 6.30: Temperature Plot: Anti-sunside

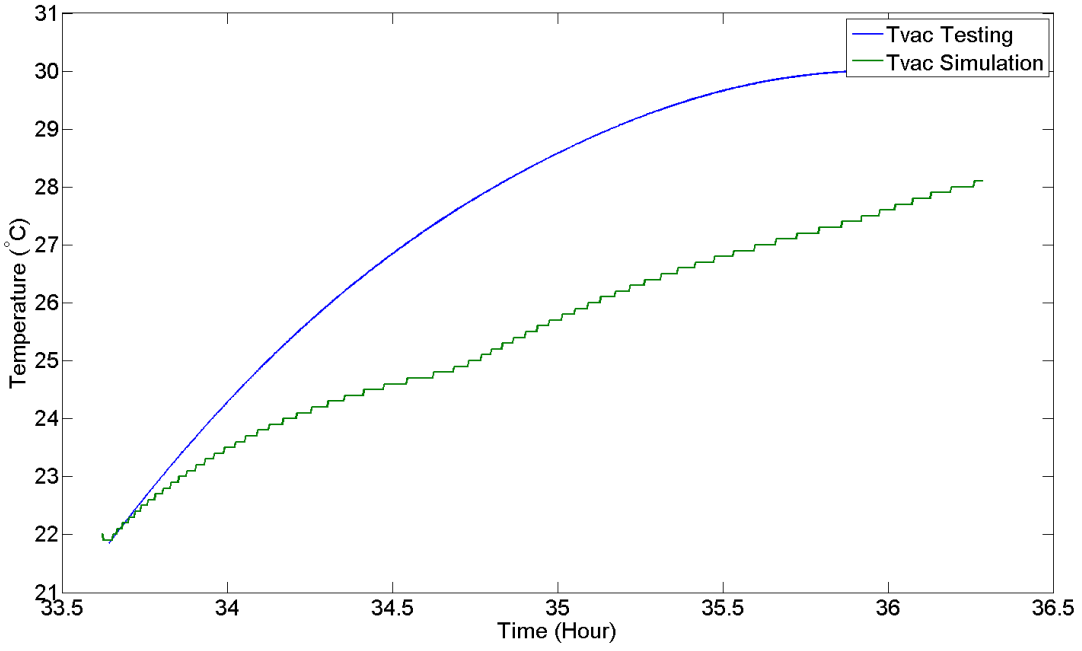


Figure 6.31: Temperature Plot: Battery

**Inferences:**

1. Initial Temperature of a particular component in testing is not same as in simulation, because during testing, initially all the components were at different temperature while in simulation initial temperature of components was set to 24 $^0$C.

2. Shape of temperature profiles are similar, but time lag can be seen. Time lag is relatively more for inner components (Communication boards) than outer components (Solar Panels).

3. Time lag mentioned above can be explained due to following reasons:

   (a) Wires used for temperature measurement by thermistors caries analog signals. And in our case length of wires used were longer than it should be for analog signal transfer causing time lag in data storage.

   (b) Thermistors were not mounted properly on the components which can cause time lag too.

   (c) Screws, Stubs and surface contacts have been modeled by total conductance which were calculated assuming, contacts are thermally ideal. But, in reality it never happens. So, in simulation, total conductance was more than that in testing. Which can explain pots of internal components. When snap was done after 5 hours beacon board experienced a temperature-kick before cooling down. This temperature-kick can be observed in case of simulation too, but of less magnitude. Because total conductivity defined between Power amplifier and Anti-sunside is more in the simulation thus heat is getting out very quickly which is not the case in testing. The same can be applied for other internal components. Due to this reason peak temperature achieved is more in testing and that is why it is taking a little extra time for cooling and thus generating a time lag.

   (d) Above argument supports the observation that time lag should be more in case of inner components than in case of outer components.

# Chapter 7

# Appendix1

## 7.1 Material properties

| Property | Al T-6061 | Solar Panel | FR-04 | MLI | SS 304 |
|---|---|---|---|---|---|
| Density(kg/m$^3$) | 2700 | 2700 | 1900 | 0 | 8000 |
| Conductivity(W/m-K) | 155 | 0.192 | 0.23 | 0.05 | 16.2 |
| Specific Heat Capacity(J/kg-K) | 1256 | 755 | 1200 | 755 | 500 |
| Absorptivity | 0.2 | 0.75 | 0.65 | 0.36 | |
| Emissivity | 0.031 | 0.85 | 0.7 | 0.65 | |

Table 7.1: Material properties: Thermal

**Other values:**

- Low emittance tape = 0.05
- OSR = 0.78

## 7.2 Thermal Conductivity Values

| Object I | Object II | Connected through | Total Conductance |
|---|---|---|---|
| Solar Panel | Side | Screw and Washer | 0.014 |
| Side | Flange | Surface Contact | 1.458 |
| Side | Power Board | Stub and Screw | 0.030 |
| Side | OBC Board | Stub and Screw | 0.030 |
| Side | ADC Board | Stub and Screw | 0.030 |
| Side | Uplink Board | Stub and Screw | 0.030 |
| Side | Downlink Board | Stub and Screw | 0.030 |
| Side | Beacon Board | Stub and Screw | 0.030 |
| Side | Heat sink | Stub and Screw | 0.066 |
| PCB | Heat sink | Screw | 0.070 |
| Side | Magnetometer | Stub and Screw | 6.597 |
| Side | GPS | Stub and Screw | 0.912 |
| Side | MLI | Surface Contact | 0.007 |
| Beacon Board | Heat sink | Surface Contact | 0.790 |
| Downlink Board | Heat sink | Surface Contact | 0.790 |
| Uplink Board | Heat sink | Surface Contact | 0.605 |
| Side | Battery Box | Stub, Screw and Washer | 0.013 |

Table 7.2: Thermal Conductivity Values